

NOTE TO USERS

This reproduction is the best copy available.

UMI[®]

**Dynamic Wetting and Heat Transfer Behaviour of
Aluminium Droplets Impinging and Solidifying on Copper Substrates**

Sébastien Leboeuf
Mining, Metals and Materials Engineering
McGill University, Montreal

May 2004

A thesis submitted to McGill University in partial fulfilment of
the requirements of the degree of Master of engineering

© Sébastien Leboeuf 2004



Library and
Archives Canada

Bibliothèque et
Archives Canada

Published Heritage
Branch

Direction du
Patrimoine de l'édition

395 Wellington Street
Ottawa ON K1A 0N4
Canada

395, rue Wellington
Ottawa ON K1A 0N4
Canada

Your file *Votre référence*

ISBN: 0-494-06565-6

Our file *Notre référence*

ISBN: 0-494-06565-6

NOTICE:

The author has granted a non-exclusive license allowing Library and Archives Canada to reproduce, publish, archive, preserve, conserve, communicate to the public by telecommunication or on the Internet, loan, distribute and sell theses worldwide, for commercial or non-commercial purposes, in microform, paper, electronic and/or any other formats.

The author retains copyright ownership and moral rights in this thesis. Neither the thesis nor substantial extracts from it may be printed or otherwise reproduced without the author's permission.

AVIS:

L'auteur a accordé une licence non exclusive permettant à la Bibliothèque et Archives Canada de reproduire, publier, archiver, sauvegarder, conserver, transmettre au public par télécommunication ou par l'Internet, prêter, distribuer et vendre des thèses partout dans le monde, à des fins commerciales ou autres, sur support microforme, papier, électronique et/ou autres formats.

L'auteur conserve la propriété du droit d'auteur et des droits moraux qui protègent cette thèse. Ni la thèse ni des extraits substantiels de celle-ci ne doivent être imprimés ou autrement reproduits sans son autorisation.

In compliance with the Canadian Privacy Act some supporting forms may have been removed from this thesis.

Conformément à la loi canadienne sur la protection de la vie privée, quelques formulaires secondaires ont été enlevés de cette thèse.

While these forms may be included in the document page count, their removal does not represent any loss of content from the thesis.

Bien que ces formulaires aient inclus dans la pagination, il n'y aura aucun contenu manquant.


Canada

ABSTRACT

The present work describes an experimental set-up built to simulate dynamic wetting and heat transfer occurring in many rapid solidification processes. Tests were performed with molten aluminium droplets falling from a crucible onto a metallic substrate. A high-speed camera captured the evolution of the droplet's geometry, while thermocouples, inserted inside the metallic substrate, allowed a heat transfer analysis to be performed. Aluminium 5754 was found to have a better initial dynamic wetting and heat transfer compared to pure aluminium. An increase in the initial temperature of the substrate was associated with better dynamic wetting and heat transfer. The heat flux was also increased by the use of a polished substrate compared to a sand-blasted substrate. The use of helium increased the two aspects studied compared to air and argon atmosphere. Totally non-wetting conditions were found for droplets in an argon atmosphere with less than 0.02% O₂.

RÉSUMÉ

Ce document fournit une description d'un montage expérimental simulant le comportement de la mouillabilité dynamique et du transfert de chaleur dans les procédés à solidification rapide. Les expériences ont été réalisées à l'aide de gouttelettes d'aluminium chutant d'un creuset sur des substrats de cuivre. Une caméra haute vitesse a capté l'écrasement de la gouttelette, alors que des thermocouples insérés dans le substrat ont permis l'analyse du transfert de chaleur. L'alliage d'aluminium 5754 a démontré de meilleures performances au niveau de la mouillabilité dynamique et du transfert de chaleur initial comparativement à l'aluminium pur. Une augmentation de la température initiale du substrat a permis d'accroître la mouillabilité dynamique et le transfert de chaleur. Ce dernier a également été amélioré par l'utilisation d'un substrat poli. L'atmosphère d'hélium a augmenté les deux aspects étudiés, comparativement aux résultats obtenus dans l'air et l'argon. Une complète non mouillabilité a été retrouvée lors de l'utilisation d'une atmosphère d'argon ($\geq 0.02\% \text{ O}_2$).

ACKNOWLEDGEMENTS

This project was a collaboration between the Aluminium Technology Centre of the National Research Council of Canada and the McGill Metals Processing Centre of McGill University. This venture was a wonderful experience and would not have occurred without the help and confidence of my supervisors: Doctor Dominique Bouchard (Aluminium Technology Centre), Professor Roderick I.L. Guthrie and Doctor Mihaiela Isac (McGill Metals Processing Centre, McGill University). I have a profound respect for these people. Their wisdom and wide knowledge are only equalled by their great human qualities. I especially want to thank Dominique Bouchard who developed this incredible project and agreed to be my industrial supervisor.

I would like to thank Jean-Paul Nadeau for his precious help in building the set-up and to support in solving the problems that occurred throughout the project. I also thank Daniel Simard, Christian Corbeil, Maude Larouche and Helen Campbell for their technical support and guidance.

I would like to acknowledge: Jinsoo Kim for his idea of a 2D heat flow model in the substrate and for his advices, Jean-Pierre Martin and François Hamel for the discussions we had, Trevor Lewis from Alcan Inc. for providing me with AA5754 alloy, Centre québécois de recherche et de développement de l'aluminium (CQRDA) and Fonds Nature et Technologies (NATEQ) for financial support, and Claude Lalande and Blaise Labrecque for solving the administrative details that went along with it. Finally, I want to thank everyone in Aluminium Technology Centre for their kindness and encouragement.

TABLE OF CONTENTS

1. INTRODUCTION	1
2. LITERATURE REVIEW	3
2.1 – Review of rapid solidification processes for which dynamic wetting and heat transfer are important aspects	3
2.1.1 – <i>Substrate Casting Processes</i>	4
2.1.2 – <i>Surface Treatment Processes</i>	6
2.2 – Wetting	8
2.2.1 – <i>The use of the sessile drop technique to study metals wetting</i>	8
2.2.2 – <i>Set-up using the drop-splat experiment to evaluate dynamic wetting</i>	9
2.3 – Heat transfer	12
2.3.1 – <i>Inverse heat conduction problem applied to metal solidification in strip casting</i>	12
2.3.2 – <i>Experimental set-up using the drop-splat experiment to evaluate heat transfer</i>	13
3. THEORY	15
3.1 – Dimensionless numbers	15
3.1.1 – <i>Reynolds number</i>	15
3.1.2 – <i>Froude number</i>	16
3.1.3 – <i>Weber number</i>	17
3.2 – Wetting : Static Conditions	20
3.2.1 – <i>Young’s Equation</i>	21
3.2.2 – <i>Young-Dupré’s Equation</i>	23
3.3 – Wetting: Dynamic Conditions	24
3.3.1 – <i>Apparent Contact Angle Evolution</i>	25
3.3.2 – <i>Drop-splat experiment using an inclined substrate</i>	27
3.4 – Heat Transfer	29
3.4.1 – <i>One Dimensional Transient Heat Conduction Equation</i>	29
3.4.2 – <i>Inverse Heat Conduction Problem Method</i>	31
4. EXPERIMENTAL PROCEDURES	34
4.1 – Procedures	34
4.2 – Description of experimental set-up	35
5. RESULTS AND DISCUSSION	41
5.1 – Overview of results obtained	41
5.2 – Role of alloy composition of droplets on heat transfer and dynamic wetting	45

5.3 – Role of the initial temperature of the substrate on heat transfer and dynamic wetting	48
5.4 – Role of the substrate surface condition on heat transfer and dynamic wetting	52
5.5 – Role of different atmospheres on heat transfer and dynamic wetting	56
6. CONCLUSIONS AND RECOMMENDATIONS	59
6.1 – Conclusions	59
6.2 - Recommendations	60
7. REFERENCES	62
APPENDIX – Conference of metallurgists of CIM, Vancouver, 2003	67

1. INTRODUCTION

Wetting and heat transfer are two important aspects of rapid solidification processes. Such processes include strip casting, thermal spraying, laser cladding, and ribbon casting. In twin-roll strip casting, they have a major impact on the characteristics of the final product and on the productivity of the process. Recently, the Aluminium Technology Centre (ATC) has undertaken a research program to evaluate the castability of aluminium and its alloys with a vertical twin roll caster. In this process, liquid aluminium wets the surface of two rotating rolls that are water-cooled and heat is transferred so as to solidify strips. Improper wetting and/or heat transfer can result in non-uniform solidification and surface cracks; it is therefore important to properly control the two. Testing different parameters directly on a twin roll caster would be a good way to find the optimum conditions for dynamic wetting and heat transfer, but each trial is costly and allows for the experimentation of only one or two parameters at the time.

Small-scale laboratory set-ups can be used to characterize wetting and heat transfer. For example, wetting between a liquid and a solid is often studied using the sessile drop technique. The wettability is determined by measurements of the contact angle between a liquid droplet and a solid substrate [6]. However, these experiments require thermodynamic equilibrium to be established: a time scale of 100 seconds, or more, is normally necessary to make such measurements. These conditions do not reflect those found in rapid solidification processes where there is an absence of equilibrium. For example, in twin roll casting, liquid metal is in contact with the rolls for a period in the order of 1 millisecond before it solidifies and wetting thus occurs under dynamic, rather than static conditions.

The objective of this project is to build a set-up that allows for the simultaneous study of dynamic wetting and heat transfer, and to study how the two are interrelated. Such a set-up will also provide a greater understanding of conditions required to improve the casting of aluminium strips. In this work, conditions that affected dynamic wetting were identified and the corresponding heat transfer was characterized. The different casting

conditions that were studied were: gaseous atmospheres, composition of the alloys studied, surface condition and initial temperature of the substrate. A literature review, an overview of the theory, and a description of the experimental procedures are given prior to the analysis and discussion of results.

2. LITERATURE REVIEW

2.1 – Review of rapid solidification processes for which dynamic wetting and heat transfer are important aspects

Rapid solidification processes are of great interest in the metallurgical field. Various techniques are employed to obtain rapid solidification of molten metals and some reviews have been written on the subject by Collins [1], Fleetwood [2], Jacobson et al. [3], and Ohnaka [4]. According to the Metals Handbook [45] rapid solidification is: “The cooling or quenching of liquid (molten) metals at rates that range from 10^4 to 10^8 °C/s.” Collins [1] and Jacobson et al. [3] do not strictly consider the cooling rate as being a factor of classification. These reviews indicate that the key factor to classify a solid metal as being rapidly solidified is the appearance of a different microstructure of the one obtained using classical casting processes. Systems showing cooling rates of 100 K/s were found to have similar properties when a precise control of nucleation was done. Indeed, the objective of rapid solidification processes is to control the solidification in a melt undercooled as much as possible under the equilibrium temperature. Because it is very difficult to melt metals totally free of contaminants, and so of nucleation sites, rapid solidification processes are used to cool the melt rapidly so as to obtain a large undercooling before nucleation sites have had the time to develop to a critical size.

Many advantages exist in using rapid solidification processes. Most relate to the enhancement of properties. Their improvement is linked to the microstructure obtained. For instance, the resulting material has smaller grain sizes and a refinement of segregation patterns (smaller cells and/or dendrites). These enhance chemical homogeneity, strength modulus, corrosion resistance and magnetic properties. It has also been shown that a higher solid solubility can be obtained. For instance, the solid solubility of iron in aluminium alloys was increased from 0.03% to 4 at. % using rapid solidification [1]. Metastable phases are created and sometimes, crystallisation can be avoided, leading to non-crystalline, or “glassy” alloys.

In spite of these positive features, the main factor that has really contributed to help commercialisation of rapid solidification processes is the gain in productivity. The use of these processes can sometimes eliminate the need for extra processing. For instance, a strip caster, twin roll and/or single belt caster, producing metals strips of 1 to 5 millimetres thick directly from the melt, can significantly reduce the need for a hot rolling mill.

For aluminium alloys, the benefit of using rapid solidification is similar to other metals with the improvement of properties mentioned earlier such as mechanical properties, solid solubility and grain refinement. Monteiro [5] studied the influence of rapid solidification on mechanical properties and grain size. He concluded that the mechanical properties (ultimate tensile strength, elongation percentage, and microhardness) were improved by a factor of up to two for some alloys when they were rapidly solidified using the melt-spinning process. The grain size was also lowered and the resulting improvements were coupled with economical benefits due to the increase in productivity. In summary, the use of rapid solidification processes proved to be valuable on the property level of the solidified metals and on the production cost.

Different processes exist to obtain the desired cooling rates. A classification was done by Collins [1] and it includes substrate casting processes, surface melting processes, as well as atomization processes. Most of the atomisation processes do not require the metal to wet a surface. Since the objective of this project is to study the interaction of dynamic wetting and heat transfer, these processes will not be included in the following discussion.

2.1.1 – Substrate Casting Processes

Substrate casting processes are certainly the most widely used in rapid solidification processes. In this family of processes, molten metal is brought into contact with cooled substrates. Many industrial processes are using this technology and this section will focus on three of them; the melt spinning processes, the single belt caster and the twin-roll caster.

The melt spinning processes (see Figure 2.1) is in fact a family of processes since a wide variety are based on its principle where a small stream of molten metal is brought into contact with a rotating cooled wheel. These are called: chill block melt spinning, free jet melt spinning and planar flow casting. The melt spinning apparatus normally produces thin ribbons of typically 5 millimetres wide. Cooling rates of 10^5 to 10^6 K/s can sometimes be reached for thin sections of 15-100 μm . This technique is used to produce long and continuous sheets of steel, aluminium, copper, titanium based alloys and superalloys. Due to the very thin sections produced, simultaneous control of the dynamic wetting and the interfacial heat transfer is crucial in order to obtain good results.

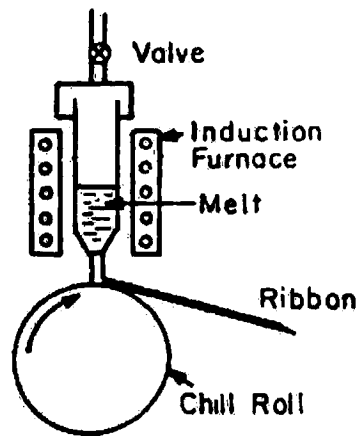


Figure 2.1 – Representation of the melt spinning process [1]

Dynamic wetting and heat transfer are also important for the single belt caster. This second process is not yet commercially used, but should be in a near future. Figure 2.2 is an illustration of a single belt simulator as the one built in McGill Metals Processing Centre in McGill University. It consists of a cooled moving substrate on which molten metal solidifies to form a strip at a velocity of 0.3 to 1.2 m/s.

In the twin roll process, molten metal is solidified into a strip using water-chilled rolls. The rolls can be made of copper, steel or any type of material judged adequate. Due to the high cooling rates and short metal/mould contact time, conventional set-ups, such as the sessile drop method, cannot be used to simulate the wetting phenomena existing at the interface. Setting up an appropriate experiment can provide precious information on the

optimum parameters to use, such as the composition of the gaseous atmosphere or the substrate material, and this was one objective of the current research program.

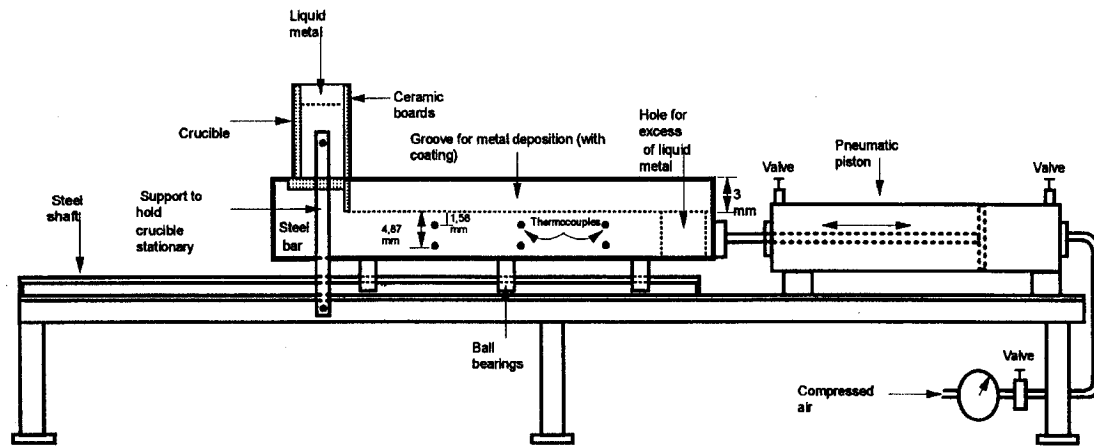


Figure 2.2 – Representation of the single belt simulator build in McGill University [28]

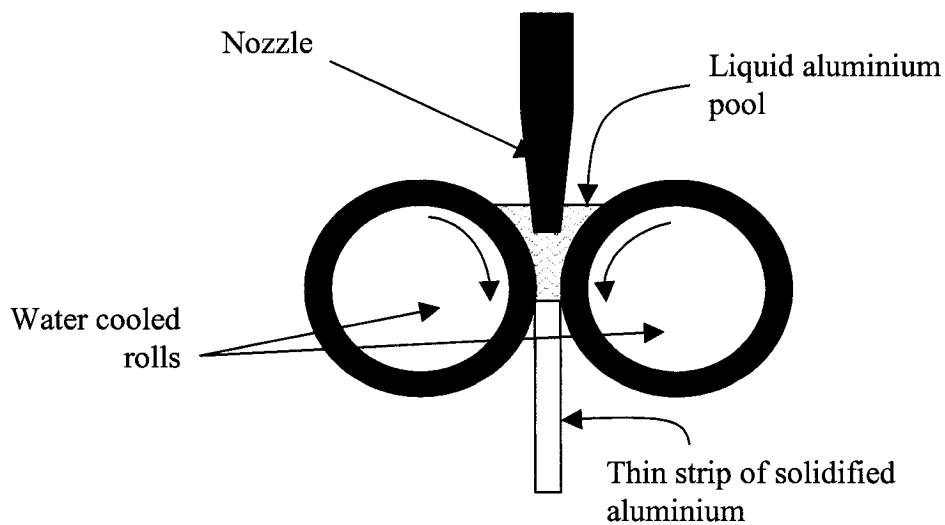


Figure 2.3 – Representation of the vertical twin roll caster of IMI

2.1.2 – Surface Treatment Processes

Surface treatment processes are those where the substrate surface is melted and/or where metal powders are melted and deposited on the substrate. Therefore, plasma spraying,

thermal spraying, spray casting, laser cladding and electron beam, fit in this category. Figure 2.4 is a representation of the thermal spraying process; the principle is somewhat similar for the other processes mentioned. In these processes a pressurized gas, at high temperature, carries (or not) powders that are melted and then impinged on a substrate. The substrate is then coated, its surface melts and mixes in with the molten particles. For plasma spraying, the particles are projected onto a rough substrate, but the substrate's surface is not melted as in some other processes.

Surface treatment processes are among those with the highest cooling rates that can be reached. For instance, in laser cladding, no interface exists between the molten metal and the solid substrate. Also, the thickness of molten material is relatively small compared to the substrate surface, which acts as a heat sink. Therefore the heat transfer is very rapid and cooling rates of up to 10^7 to 10^8 can be achieved. Cooling rates are not as high for plasma spraying, but interfacial effects are nevertheless negligible due to the high impact velocity of the molten particles. Once again dynamic wetting and heat transfer are important since the spreading of particles (plasma spraying), the contact quality at the interface and the cooling rates depend on it.

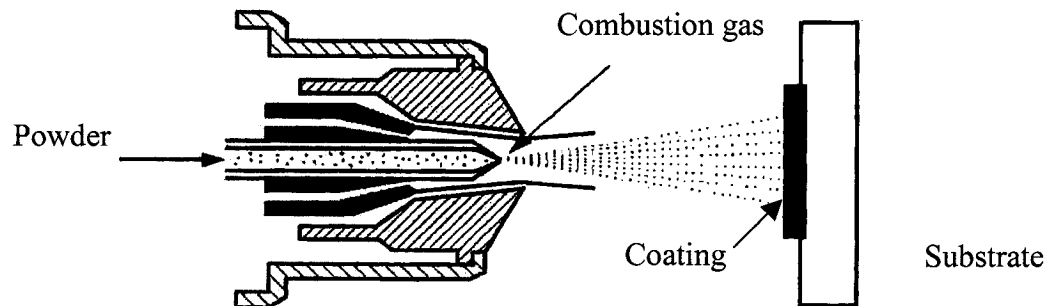


Figure 2.4 – Representation of thermal spraying process [50]

2.2 – Wetting

2.2.1 – The use of the sessile drop technique to study metals wetting

The sessile drop technique is a widely used method to study metals wetting a given surface. The number of papers dealing with this technique is incredibly large. Reviews have been written by Eustathopoulos et al. [6,7,8], Blake [9] and Good [10], to name a few. The sessile drop method is generally employed to determine the contact angle between a liquid and a substrate, or to determine the value of a liquid's surface energy σ_{LV} (see section 3.2.1). With this method, one has to use a flat horizontal substrate, a chamber with a controlled atmosphere, equipment to melt the metal or to heat the system to a predetermined temperature and a facility to provide a way of measuring the shape of the droplet and of the contact angle. The liquid droplet is either dropped or melted on the substrate and images are recorded until equilibrium is reached.

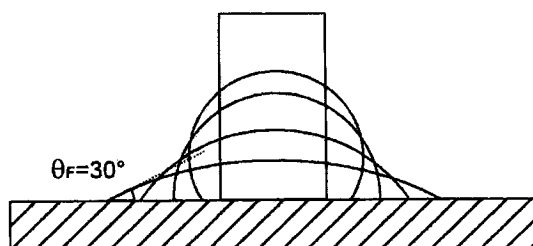


Figure 2.5 – Schematic illustration of the profiles assumed as a solid cylinder melts to form a sessile drop [6]

In the present project, some of the relevant papers on the sessile drop technique were written by Xue et al. [11], Ho et al. [12], Wu et al. [13], and Landry et al. [14]. These authors studied the wetting of aluminium on different surfaces such as boron nitride, sintered aluminium nitride, sapphire, and carbon respectively. One important point outlined by every author was the need to perform the experiments under highly controlled atmospheres (either high vacuum or pure inert gas) so as to decrease the oxidation of aluminium (which is virtually impossible to avoid).

Although these papers are all related to aluminium wetting some surfaces, the link with the present study is not strong. For the actual project, the aluminium is wetting a copper substrate and an oxide layer is covering the substrate. Therefore the existing system is an oxidized molten metal over a metal oxide. Also the whole system is non-reactive, that is, the aluminium is not chemically reacting with the copper substrate. Gallois [15] summarized the state of such a system. Pure liquid metals and an oxidized interface are generally characterised by non-wetting conditions. Using the sessile drop method, Gallois [15] showed that the oxygen dissolved in the metal could significantly improve the wetting of pure metals over oxidized surfaces. This result will be discussed in an upcoming chapter. Finally, Ueda et al. [16] studied the influence of the droplet size on the contact angle between liquid iron and alumina. They showed that the droplet radius had an influence upon the contact angle.

In general, valid static wetting experiments have to meet some specific criteria as stated by Eustathopoulos et al. [6] and summarised by Ebrill [17]. The experiments must be done with: clean solid and liquid surfaces, isothermal conditions, negligible or at least controlled, roughness of solid substrate and negligible external forces (impact energy). These conditions are generally not present in industrial scale rapid solidification processes. Consequently, another experimental approach had to be used to evaluate dynamic wetting and it was found that the drop splat experiment would better simulate the conditions found in the processes.

2.2.2 – Set-up using the drop-splat experiment to evaluate dynamic wetting

Several authors have used the drop-splat experiment used in this project to evaluate the dynamic wetting and the effect of various parameters. Set-ups used were not identical to each other, but the end result: to study dynamic wetting using molten metal droplets impinging on a given substrate, was the same.

Adler et al. [18] were among the first to acknowledge the importance of dynamic wetting in solidification processes. Their objective was to characterize the dynamic wetting interaction and the solidification behaviour of a solidifying metal and a substrate during

melt spinning process. Their experimental approach was to produce droplets of various compositions that would impact on an inclined copper substrate after a short free-fall. These experiments were performed in a vacuum in order to reduce the effect of a boundary layer that may exist between the liquid metal and the solid, heat removing, substrate. The use of a high-speed camera allowed the impact phenomena and solidification to be observed. According to Adler et al. [18], the use of classical sessile drop wetting procedures was not possible due to the unusual shape of the spreading droplet.

Maringer [19] used a similar approach to study rapid solidification techniques. His objective was to evaluate the effect of the initial temperature on dynamic wetting and the adhesive bond existing between the molten metal and the substrate. Droplets were made to impact on a substrate inclined at a fixed value. He found that for substrate temperatures higher than a critical value, T_{crit} , the droplets began “sticking” to the substrate surface. The adhesive bond existing at the droplet/substrate interface explained this.

Dong et al. [20] studied the deformation of melts (pure Pb, Bi, Sn and alloys) on a chill substrate during solidification. They studied this phenomenon using a camera operating at 500 to 1000 frames/second. The authors concluded that the instantaneous deformations of solidifying metals could explain the presence of certain defects on the cast surfaces of some rapid solidification processes.

Some authors working in the field of coatings (thermal and plasma spraying, hot dip coating, and others) used the drop-splat experiment to study the interaction of molten metal with cooled substrates. Ulrich et al. [21] melted metallic rods of tin, lead, aluminium and steel, using an infrared heater or induction coil to form molten droplets and have them impinge on a solid surface. They studied the effect of impact velocities on the splat after the impact. The authors characterised the dynamic wetting using high-speed imagery to determine the spread factor. This factor was found to increase with increasing impact velocities, which meant that the spreading of the droplets over the surface was increased by the higher kinetic forces acting on them.

Amada et al. [22] studied the influence of wettability on the flattening ratio of droplets. Spread factor and final contact angles were measured for different heights of fall and droplet sizes. The flattening ratio was plotted against Reynolds and Weber numbers. Flattening ratio was found to depend upon wettability and the dimensionless numbers mentioned above, through the weight of the droplets and their height of fall.

Nishioka et al. [23], who were also working in the thermal spraying field, studied the effects of the initial temperature of the substrate on droplet morphology, being splash type or disk type. Droplets were dropped onto gold-coated steel substrates in nitrogen at atmospheric pressure and under low-pressure conditions. The authors found that wetting played a dominant role in the flattening of the droplet. They also studied the droplet's microstructures and found that the grain size decreased as the temperature of the substrate was increased.

Ebrill et al. [17, 24-26] studied both dynamic wetting and interfacial heat fluxes using two different set-ups. For dynamic wetting, they used an experimental apparatus similar to those cited above and the evolution of the wetting angle of the solidifying droplets was captured using a high-speed camera. Using 25-50 milligram droplets, falling from three to six millimetres in a reducing 5% H₂/N₂ atmosphere, the authors demonstrated the influence of initial temperature of the substrate on dynamic wetting; the latter being improved as the substrate temperature approached the melting point of the molten metal. To characterise wetting, Ebrill et al. [17, 24-26] used the apparent evolution in contact angle, which will be discussed in another chapter (see section 3.3.1).

From the literature review of work using the drop-splat experiment to study dynamic wetting, it can be stated that three methods have been employed to evaluate the dynamic wetting: 1) evaluation of the apparent contact evolution, 2) the drop-splat experiment with inclined substrate and 3) the spread factor. The various parameters studied by the authors were the height of fall of the droplets, the weight of the droplets, the temperature of the substrate and the composition of the molten metal.

2.3 – Heat transfer

2.3.1 – Inverse heat conduction problem applied to metal solidification in strip casting

The second aspect needed for the accomplishment of this project was the evaluation of the heat transfer. Diverse techniques are employed to determine heat fluxes in solidifying metals, but the leaders in the field of metal solidification usually treat the subject as an *inverse heat conduction problem* (IHCP). Among the various techniques to solve this family of heat transfer problems, the *sequential function specification method*, developed by James V. Beck [27], is often used. This method was employed by Professor Roderick I.L. Guthrie's team at the McGill Metals Processing Centre to evaluate heat fluxes in different casting equipment. Kim et al. [28] used the IHCP to calculate heat fluxes and heat transfer coefficients on a single belt casting simulator (see section 2.1.1) for two types of aluminium alloys, AA5754 and AA5182. Increases in strip thickness and in superheat were both found to increase the maximum heat fluxes during solidification. Tavares et al. [29] used the IHCP to characterise the interfacial heat transfer for the solidification of low-carbon steels on a twin-roll caster. Evaluation of the secondary dendrite arms spacing (SDAS) was performed on the strips. The authors demonstrated that the experimental values for instantaneous interfacial heat fluxes were in good agreement with the SDAS. Finally, Guthrie et al. [30] also used the IHCP to study interfacial heat fluxes for single belt and twin-roll casters. Several parameters have been successfully studied and showed the good performance of the inverse heat conduction problem applied to strip casting apparatus.

Authors working with experimental set-ups reproducing the casting conditions also used various IHCP methods to calculate heat fluxes. Strezov et al. [31, 32] and Bouchard et al. [33, 34] both have built dip testers to evaluate the influence of different parameters on the interfacial heat fluxes and/or interfacial heat transfer coefficients. Metallic substrates with thermocouples embedded were dipped into liquid baths of stainless steel (Strezov) and copper (Bouchard), in order to simulate conditions existing at the roll/melt interface in the twin-roll strip casting process. Muojekwu et al. [48] applied the same technique to a similar set-up to study the solidification of aluminium alloys (1D).

Finally, the IHCP method was also employed by Todoroki et al. [39, 40, 41] and Misra et al. [35] to measure the interfacial heat fluxes in a set-up similar to the drop splat experiment used in this study. IHCP was treated as a one-dimensional problem. The technique showed good results and was applied in the present investigation.

2.3.2 – Experimental set-up using the drop-splat experiment to evaluate heat transfer

Many types of set-ups can be employed to measure the interfacial heat transfer between a solidifying metal and a substrate. Among them, the drop splat experiment is probably one of the least expensive to operate for studying heat transfer. It was seen in section 2.2.2 that the drop splat was also used to characterize dynamic wetting. The drop-splat set-ups for dynamic wetting experiments have also been used to characterize heat transfer. This section is devoted to a review of the few existing drop splat set-ups that have been used to evaluate interfacial heat fluxes. Liu et al. [36, 37] and Wang et al. [38] used an electromagnetic levitator to melt 0.4 to 1 gram nickel droplets. The droplets fell from heights of 265 to 365 millimetres. A pyrometer was used to measure the top surface temperature of the splat after impingement. The authors, who were working in the splat cooling and spray deposition field, studied the effect of superheat, substrate materials and surface condition, on cooling rates and interfacial heat transfer.

Todoroki et al. [39-41] inserted thermocouples inside the substrates to measure the temperature evolution as the droplets solidified and evaluated the interfacial heat transfer coefficients along with heat fluxes. Droplets of steel, pure iron, and nickel were made to impact on the substrate after having been ejected from a quartz nozzle. Surface conditions of the substrates, superheat of the molten metals and alloy compositions, were found to influence the heat transfer. Also, one important thing pointed out by the authors was that the maximum heat flux was highly depending on the position of the impingement point of the droplet. Maximum heat fluxes were found for droplet falling directly above the inserted thermocouples. Any displacement of the impact point would result in lower heat fluxes.

Loulou et al. [42, 43] also used thermocouples embedded in the substrate to measure heat fluxes, but they used a semi-intrinsic method (see section 4.2) to obtain a faster and better time response for their temperature readings. They studied 3.5 grams tin, lead and zinc droplets falling from 15 millimetres high on the nickel substrates. The effects of substrate roughness and melt superheat were studied. Also, the use of different lubricants at the substrate surface showed that the heat transfer was improved when the micro cavities existing at the interface were filled with grease or oil, the contact resistance being then decreased. Finally, Loulou et al. [42, 43] were among the first to make a link between heat fluxes and wetting. They found that metals with lower surface tensions and contact angles were showing better performance for the heat transfer. However, the surface tension and contact angles values were taken from other publications and were then not measured simultaneously with the heat transfer.

Evans et al. [44] also showed the importance of wetting on heat transfer. Although no direct wetting measurements were taken, they showed that an increase in the surface tension of steel droplets was associated with a decrease in the maximum heat fluxes. To do so, they used a levitation apparatus with 0.7 grams droplets. Temperature measurements were once again performed using thermocouples.

In summary, the parameters studied by the authors using the drop splat experiment to analyse heat transfer were: melt superheat, melt composition, substrate material, substrate roughness, presence of a lubricant at the substrate surface, and location of the impingement point.

Although it has been shown that the drop-splat set-up is suited to study dynamic wetting and heat transfer at the initiation of solidification, the set-up has never been used to analyse the two phenomena during the same experiment. It is often assumed that improved dynamic wetting promotes heat transfer but this is best demonstrated by simultaneously characterizing both phenomena.

3. THEORY

3.1 – Dimensionless numbers

Dimensional analysis and physical similarities are of great use in the field of metals casting technology [53]. One can reproduce the existing conditions of some given processes through set-ups of variable dimensions. These models can be used to study the influence of process parameters without having to perform the experiments directly on full-scale equipment. When physical similarities exist between the prototypes and their models, optimum conditions obtained from the tests may be applied directly to the existing processes and should behave the same way. Apart from practical purposes, the use of small-scale equipment is also justified by economic advantages and timesaving [58].

In order to evaluate physical similarities and/or dimensional analysis, it is crucial to have some knowledge of the forces acting in the system studied. In the present study, when a droplet falls and impinges on a substrate, the main forces that are present are as follows: inertial, viscous, gravitational and surface tension. The ratio of these forces over the inertial forces will give rise to three numbers that are more likely to appear in many fluid flow studies, i.e., Reynolds number, Froude number and Weber number.

3.1.1 – Reynolds number

The Reynolds number is widely known and used in fluid dynamics. For instance, it is used in closed pipe studies to determine the nature of a fluid flow (turbulent or laminar). The Reynolds number (Re) is given by the ratio of inertial forces over viscous forces:

$$\text{Re} = \frac{|Inertial\ forces|}{|Viscous\ forces|}. \quad (3.1)$$

Here, inertial forces are proportional to the mass (m) of the fluid on which it acts multiplied by the acceleration (a) of this fluid:

$$Inertial\ forces \propto ma, \quad (3.2)$$

where the mass is the density of the fluid (ρ) multiplied by its volume (l^3) and the acceleration is the rate of change of the velocity (u) of the fluid with time (t):

$$m = (\rho l^3); \quad a = \frac{u}{t}; \quad u = \frac{l}{t} \text{ or } t = \frac{l}{u}. \quad (3.3 \text{ a to d})$$

Making the appropriate substitution, equation 3.2 becomes:

$$\text{Inertial forces} \propto (\rho l^3) \left(\frac{u}{t} \right) = \frac{\rho l^3 u}{l/u} = \rho l^2 u^2. \quad (3.4)$$

Viscous forces are produced by the shear stress existing between the fluid “layers”, which is the product of the viscosity (μ) of the fluid and the rate of shear (u/l) and acting on a surface l^2 , therefore:

$$\text{Viscous forces} \propto \frac{\mu u}{l} l^2 = \mu u l. \quad (3.5)$$

Combining these equations, we obtain Reynolds number:

$$\text{Re} = \frac{|\text{Inertial forces}|}{|\text{Viscous forces}|} = \frac{\rho l^2 u^2}{\mu u l} = \frac{\rho l u}{\mu}. \quad (3.6)$$

The Reynolds number is of great importance in characterizing fluid flow through pipes or flows that pass around submerged objects, but in the present case, viscous forces are not the main forces acting on the droplets and the use of Reynolds number is not the most relevant.

3.1.2 – Froude number

Gravity forces also have a role to play in fluid dynamics. The Froude number (Fr) is a dimensionless number that expresses the role of the gravity forces relatively to the inertial forces. Therefore,

$$Fr = \frac{|\text{Inertial forces}|}{|\text{Gravity forces}|} \quad (3.7)$$

where gravity forces are expressed using the weight of a particle:

$$\text{Gravity forces} = mg = \rho l^3 g. \quad (3.8)$$

With the inertial forces given by equation 3.4 and making the appropriate substitution for the gravity forces, Froude number is proportional to:

$$Fr = \frac{|Inertial\ forces|}{|Gravity\ forces|} \propto \frac{\rho l^2 u^2}{\rho l^3 g} = \frac{u^2}{lg}. \quad (3.9)$$

Every flow that has a free surface is influenced by gravity forces, since pressure forces are constant everywhere. Therefore, flows like ocean waves or casting streams are related to Froude number, but for droplets impinging on a substrate in free fall conditions, the gravity forces are included in the velocity term (u) since the droplet's final velocity depends on its weight and its height of fall. That leads to the last combination of forces acting on the system, inertial forces and surface tension forces.

3.1.3 – Weber number

Surface tension forces are often negligible in the evaluation of metallurgical processes, but coupled with inertial forces, it plays an important role in the evolution of the shape of the droplet as it collides with the substrate. Surface tension forces act at a fluid's surface and are responsible for holding the fluid together. The ratio of inertial to surface tension forces is given by the dimensionless Weber number (We) expressed as:

$$We = \frac{|Inertial\ forces|}{|Surface\ tension\ forces|} \propto \frac{\rho l^2 u^2}{\sigma l} = \frac{\rho l u^2}{\sigma}. \quad (3.10)$$

This number is the most representative of the three presented above. In the evaluation of wetting, surface tension is the predominant characteristic (see section 3.2). In rapid solidification processes, the forces acting on the fluid can vary over a wide range and Weber number will vary accordingly at surfaces such as triple point.

Table 3.1 – Thermophysical properties of liquid aluminium [55]

	<i>density</i> (ρ)	<i>Viscosity</i> (μ)	<i>Surface tension</i> (σ)
$660^\circ C$	2380 kg/m ³	1.90 mPa s	0.914 N/m
$725^\circ C$	2360 kg/m ³	1.90 mPa s	0.892 N/m

In equation 3.10, ρ is the density of the fluid, l corresponds to the diameter of the droplet, u is the velocity of the droplet at the moment of impact/contact with the substrate and σ is the surface tension of the liquid. The density and the surface tension of aluminium are

known and shown on Table 3.1. The other values are related to the volume of the droplet and the height of fall; these values have to be determined using different physics relations. The diameter of the droplet l is evaluated from the mass (m) of the solidified droplet,

$$m = \rho V \quad (3.11)$$

Assuming a perfect sphere when the droplet is falling (which is not necessarily always the case), the volume V of the droplet is:

$$V = \frac{4}{3} \pi R^3. \quad (3.12)$$

Since $l = D = 2R$ and combining equations 3.11 and 3.12,

$$m = \frac{1}{6} \pi \rho l^3 \quad (3.13)$$

or

$$l = \sqrt[3]{\frac{6m}{\pi\rho}}. \quad (3.14)$$

To find the velocity u of the droplet before the initial contact with the substrate, the following relationship is used:

$$u^2 = u_0^2 + 2gh \quad (3.15)$$

where :

- u_0 = initial velocity of the droplet;
- g = gravitational acceleration (9.81m/s^2);
- h = height of fall of the droplet.

Since the droplet is free-falling from the crucible $u_0^2=0$, therefore equation 3.10 becomes:

$$We = \frac{2\rho gh \left(\frac{6m}{\pi\rho}\right)^{1/3}}{\sigma}, \quad (3.16)$$

which depends on the mass of the droplet (m) and the height of fall (h). Figure 3.1 shows the combinations mass/height to obtain Weber numbers greater, equal and less than one and Table 3.2 shows Reynolds, Froude and Weber numbers for different combinations of weight and height of fall of the droplets. The dimensionless numbers were also calculated for the aluminium twin roll casting following the methodology used by Bouchard et al.

[61]. For the aluminium twin roll strip casting, the velocity term (u) was approximated to 0.4 m/s based on experimental data obtained at the Aluminium Technology Centre.

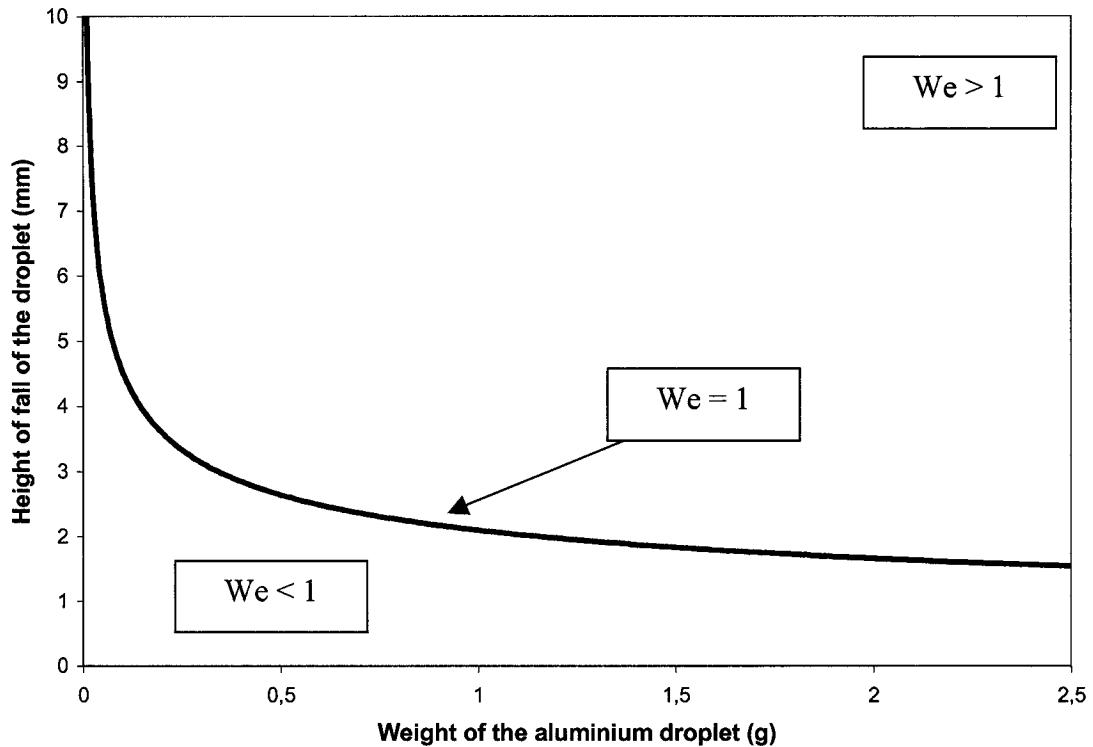


Figure 3.1 – Combinations height of fall/weight of the droplet and the corresponding Weber number values.

Table 3.2 – Values of Reynolds, Froude and Weber numbers for different combinations of weight and height of fall of the droplets compared with strip casting values

Height of fall (mm)	Weight (g)	Re	Fr	We
1	0.25	1021.37	0.34	0.30
3	0.5	2228.89	0.81	1.15
10	0.5	4069.37	2.70	3.84
10	1	5127.09	2.15	4.84
10	2	6459.72	1.70	6.09
50	0.5	9099.39	13.52	19.20
Alu. twin roll strip casting		14140.37	2.27	19.05

It is seen from table 3.2 that the parameters used in the study gives Froude and Weber numbers similar to the ones obtained in the real process. However, dimensionless numbers were not necessarily used to reproduce the existing conditions in a given process. The objective of the study was primarily to improve the understanding between dynamic wetting and heat transfer. The similarity between a process and the prototype was not sought. Weber number was used to determine the best combination of experimental parameters so that neither surface tension or gravity forces would be much greater than the other one and would have an impact on the dynamic wetting results.

3.2 – *Wetting : Static Conditions*

Wetting is defined as the capacity of a liquid to spread on a given surface (American Society of Metallurgy [45]). In metallurgy, wetting of molten metals on substrates often plays an important role. For example, in the continuous hot dip coating process for steel sheet, a zinc coating is applied to the steel sheet to improve its capacity to resist corrosion. For this process, good “dynamic” wetting of molten zinc on steel sheet briefly submerged in a bath ensures that the zinc coating will adhere to the sheet and cover the whole surface. Aluminium wetting of plastic discs for compact disc players is another example.

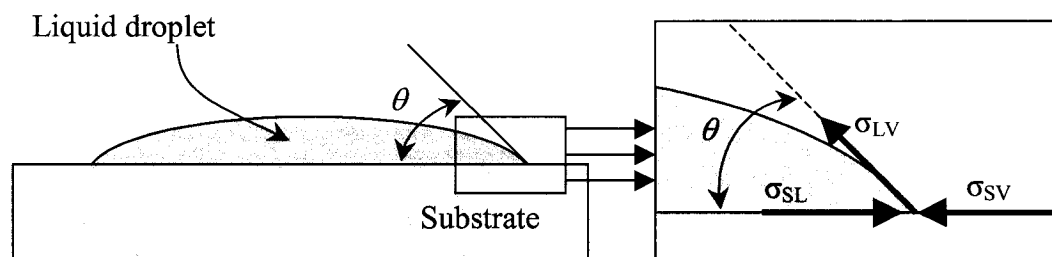


Figure 3.2 – Representation of a liquid droplet standing in equilibrium on a given substrate

Critical reviews of published work dealing with static wetting of metals on ceramics, metals or oxidized surfaces have been carried out by Eusthatopoulos [6-8] as well as by Good [10] and readers interested in this subject are invited to consult their work. Since all

experiments in this study were performed under dynamic conditions, only a general overview of wetting under static conditions is given here. This section will focus on Young's and Young-Dupré's equations.

3.2.1 – Young's Equation

Young's equation is one of the first relationships developed to explain wetting and is still of great importance in the field. Young's equation describes the behaviour of a liquid droplet wetting a perfectly flat solid surface under ideal conditions. These conditions are established only if all the following requirements are met: no net mechanical forces are acting on the liquid, no chemical reactions are occurring between the liquid and the substrate, and finally no temperature gradient exists between the two. In other words, Young's equation is valid when thermodynamic equilibrium is present.

Let us consider a liquid droplet lying on a solid surface under equilibrium conditions. Figure 3.2 is a representation of this situation. The cosine of the contact angle existing between the droplet and the substrate is described by Young's equation:

$$\sigma_{LV} \cos\theta + \sigma_{SL} - \sigma_{SV} = 0 \quad \text{or} \quad \cos\theta = \frac{\sigma_{SV} - \sigma_{SL}}{\sigma_{LV}}. \quad (3.17)$$

In this equation, θ represents the contact angle and σ_{SV} , σ_{SL} , σ_{LV} , are the energies acting at the interfaces of the solid-vapour, solid-liquid and liquid-vapour respectively. These interfacial energies meet one another on the triple line, which is normal to the surface of the printed paper. When the work provided by these energies is balanced, the system is in equilibrium and Young's equation is valid.

From this equation, it is possible to determine if the liquid wets the surface of the solid. For instance, a contact angle of 90° is used to distinguish wetting and non-wetting conditions. When the contact angle is less than 90° , the liquid is considered to wet the surface. On the other hand, if the contact angle is higher than or equal to this value, then non-wetting conditions are established. It is also stated that perfect wetting is reached

when θ equals zero. In wetting experiments, the contact angle is often used to determine the interfacial energies between the liquid and substrate.

Gibbs defined the surface energies of liquid and solid as scalar quantities representing the work needed to create reversibly new surfaces:

$$\sigma_{LV} = \left(\frac{\partial G}{\partial \Omega} \right)_{T, v, n_i} \quad (3.18)$$

$$\sigma_{SV} = \left(\frac{\partial G}{\partial \Omega} \right)_{T, v, n_i} \quad (3.19)$$

In equations 3.18 and 3.19, G is total free energy of the system, Ω represents the surface area, T is the temperature, v the volume, and n is the number of moles of the component i . Although both surface energy (σ_{SV}) and the surface tension (γ_{SV}) can be used in equation 3.17, it is important not to confuse the two. In the first case, the surface energy represents the work, by cleavage for example, that has to be done at constant strain in order to increase the number of molecules at the surface. On the other hand, the surface tension is the force that has to be performed by elastic strain to create a new surface without increasing the number of molecules (see Figure 3.3). Surface tension (γ_{SV}) of a solid is expressed by the following relation:

$$\gamma_{SV} = \sigma_{SV} + \frac{d\sigma_{SV}}{d\varepsilon}, \quad (3.20)$$

where ε is a macroscopic elastic strain. Some authors such as Ueda et al. [16] and Zhang et al. [46] incorporate a line energy term (κ) to take into account the effect of the droplet radius (R). Young's equation then becomes:

$$\sigma_{LV} \cos \theta = \sigma_{SV} - \sigma_{SL} - \frac{\kappa}{R}. \quad (3.21)$$

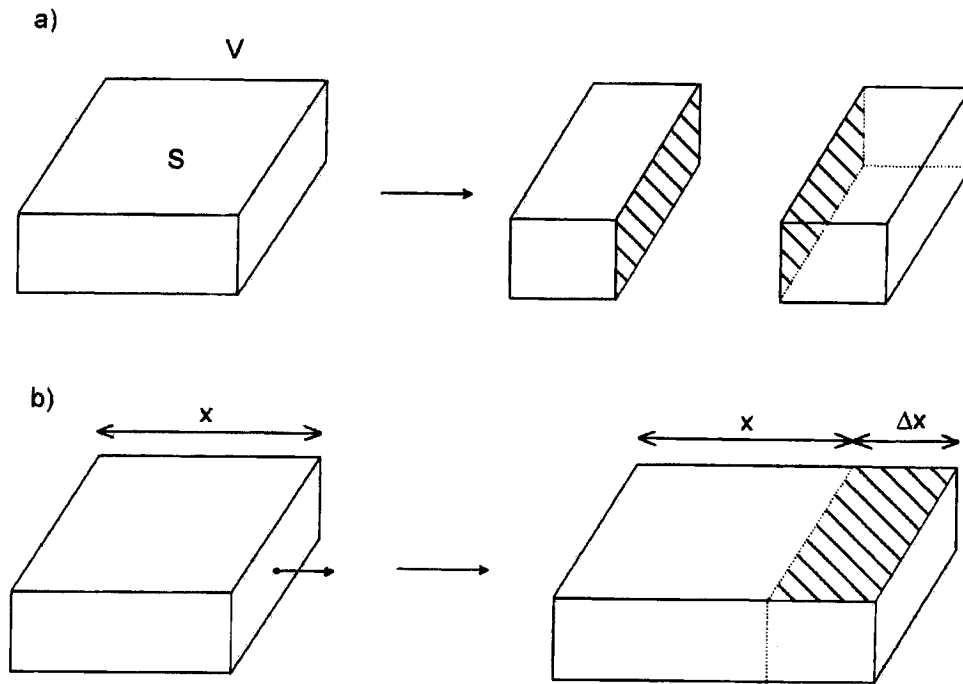


Figure 3.3 – Creation of solid surfaces (shaded) by cleavage (a) and elastic deformation (b).[6]

From Young's equation, the contact angle and the surface tension of the liquid are generally known or can be easily found. However, one problem arising from the analysis of Young's equation is that the surface energy (σ_{SV}) and the interfacial energy of the solid-liquid (σ_{SL}) are difficult to determine. Therefore one alternative solution is to use the work of adhesion (W) to develop the Young-Dupré equation.

3.2.2 – Young-Dupré's Equation

The thermodynamic value of the work of adhesion is the work necessary to separate a liquid from the surface of a solid reversibly [6]. As Gallois [15] explains, the work of adhesion is:

$$W = \sigma_{SV} + \sigma_{LV} - \sigma_{SL} \quad (3.22)$$

Rearranging Young's equation (3.17),

$$\sigma_{LV} \cos \theta = \sigma_{SV} - \sigma_{SL}, \quad (3.23)$$

and making the appropriate substitution,

$$W = \sigma_{LV} \cos \theta + \sigma_{LV} \quad (3.24)$$

or,

$$W = \sigma_{LV} (\cos \theta + 1), \quad (3.25)$$

which is the Young-Dupré equation. This equation is useful because it depends only on the surface energy of the liquid and on the contact angle. This eliminates the difficulties related to the determination of the interfacial energies of solid-liquid and solid-vapour. From this equation, it can be seen that as the contact angle rises, the work of adhesion decreases and vice versa. Therefore, a poor wetting of a liquid on a surface necessarily implies an inferior adhesion to the surface. For example, a droplet with a contact angle of 180° (totally non-wetting conditions) gives a value for the work of adhesion of zero in the Young-Dupré equation. This relationship is of great importance and it has repercussions on the dynamic wetting analysis, as will be seen in the next section.

3.3 – Wetting: Dynamic Conditions

As seen in the previous sections, there are several studies dealing with the evaluation of the static wetting of a metal over a given substrate. The techniques used, like the sessile drop technique or the transferred drop, are widely known for giving valid results. The experiments are generally performed in a controlled atmosphere with clean liquid metals and oxidation free substrates. These tests are done under complete thermodynamic equilibrium, that is, no temperature gradient, no net mechanical forces or chemical reactions between the substrate or in the droplet. Data acquisition is often made over long periods of time, several minutes and even many hours. Unfortunately, these experimental procedures do not reflect the conditions existing in the rapid solidification processes, where no equilibrium is present and where the solidifying metal is in contact with the substrate for less than a second. Therefore, new techniques had to be developed to characterize the existing conditions. This section presents three of these techniques, namely, the apparent contact angle, the adhesive bond and the spreading factor. It is important to point out that these techniques are not widely used because only a few researches have dealt with the dynamic aspects of wetting phenomena. As a result,

preliminary testing had to be performed in order to ensure the validity of these methods. The discussion includes some of these pre-test results.

3.3.1 – Apparent Contact Angle Evolution

The first procedure discussed here to evaluate the dynamic wetting was used by Ebrill et al. [17, 24-26]. The apparent contact angle evolution is a method similar in its application to the sessile drop technique. The objective is the same; that is, to measure the contact angle made between a droplet and a substrate, but the time scale used to perform the evaluation is different. For instance, in the present study, the droplets hitting the substrates took 3 to 5 milliseconds to spread on the substrate surface and the contact angle varied during 0.1 to 0.2 seconds. Consequently, it was essential to employ a high-speed camera acquiring 500 frames per second or more. The procedure was quite simple; the metal was melted and droplets were produced. A high-speed camera was recording the images from the droplet impinging the substrate. Then, each frame was analysed and the contact angle was measured on both sides of the droplet. By regrouping all the measurements together, curves similar to the ones shown in Figure 3.4 were obtained. Four droplets having the same initial conditions produced these experimental curves. At time zero, all contact angles were equal to 180° because the droplets were barely touching the substrate. Then, the angles rapidly decreasing as the droplets spread on the substrate. Once the spreading period was over, the liquid metal within the droplets tended to recoil from the substrate and the contact angle began increasing. Finally, wavy movements at the top surface of the droplet presumably caused the contact angle to vary until reaching a constant value.

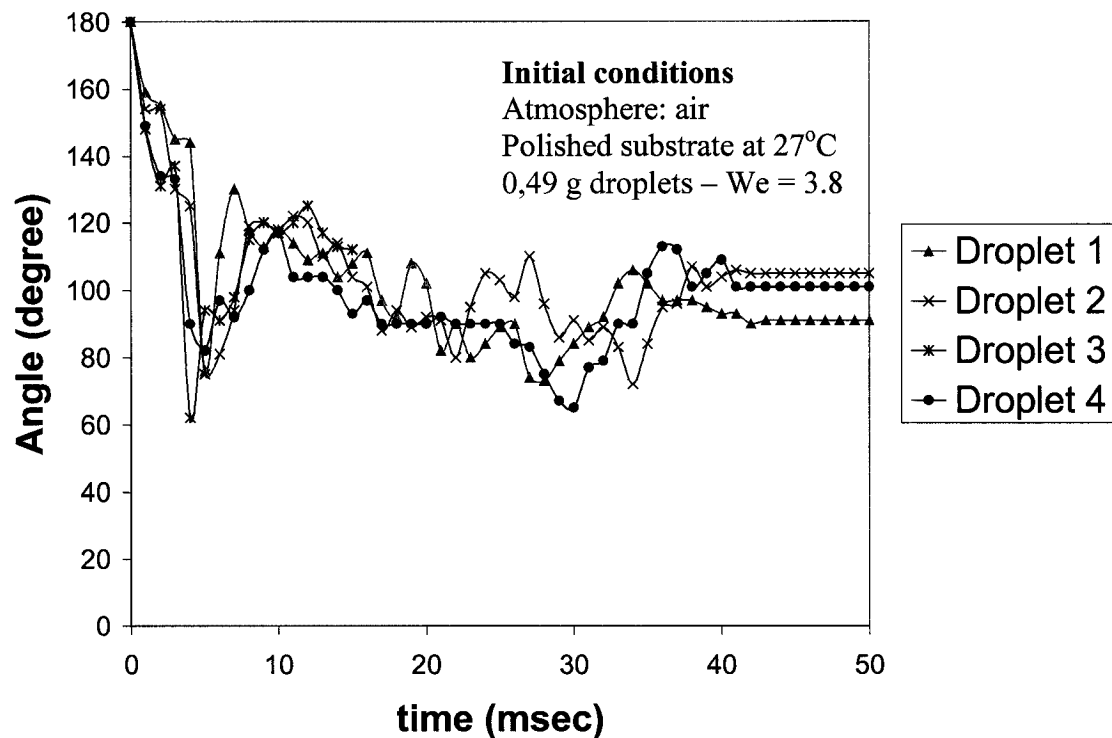


Figure 3.4 – Apparent contact angle evolution for four droplets produced using the same experimental procedures.

Although this technique was useful in terms of its resemblance to the sessile drop method, the interpretation of the results was difficult. Comparison between two curves was not an easy task. Also, another problem was the analysis of the results. More than 50 measurements had to be performed for each droplet. This analysis could then take more than a week for only one set of conditions, which is unacceptable in any industrial context. The presence of oxides at the surface of the droplet and movements of the liquid metal after the spreading of the droplet could sometimes interfere with the reading of the value and falsify the results. Ebrill et al. [17, 24-26] did not have the same problems, because they were using smaller droplets, falling from lower heights, and produced in an oxygen free atmosphere. Therefore, this method would be suitable for droplets produced with a low Weber number and a pure atmosphere, which does not necessarily reflect the existing conditions in rapid solidification processes.

3.3.2 – Drop-splat experiment using an inclined substrate

The second method studied was developed by Adler et al. [18]. The technique also implied the formation of liquid droplets and their impingement on a substrate, but this time, the substrate was inclined (see Figure 3.5). It was seen previously (section 3.2.2) that the Young-Dupré equation links the wetting of a droplet on a surface with the adhesive forces existing between the two. The technique is using this characteristic. The falling droplet was submitted to the gravity forces during its fall, but also when it hit the substrate. The force acting downward on the droplet was:

$$F = mg \cdot \sin \theta . \quad (3.26)$$

If the droplet wetted the substrate surface, then the adhesive forces would be strong enough to counteract the gravity forces and it would stick to the substrate. If not, the droplet would simply bounce back and fall off the substrate. The degree of inclination of the substrate for which the droplets started to slip was used to compare the different wetting conditions.

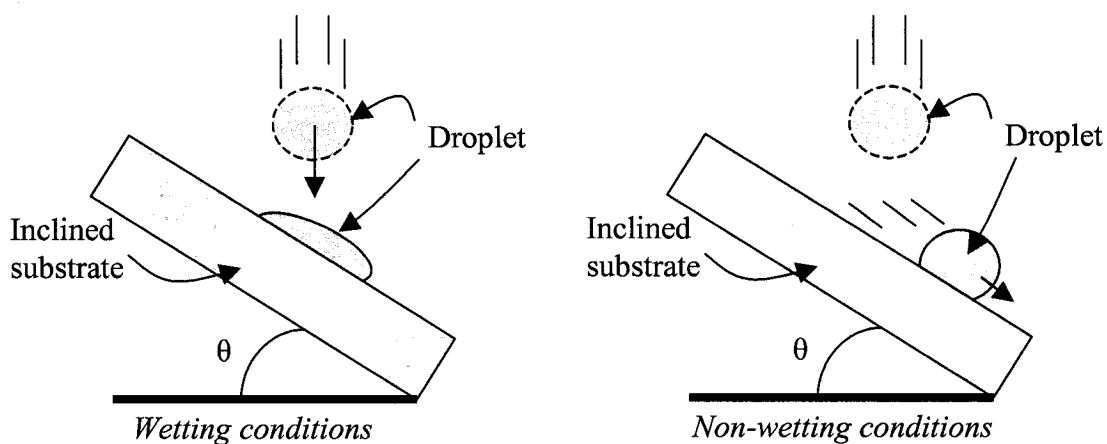


Figure 3.5 – Representation of the drop-splat experiment using inclined substrate in wetting and non-wetting conditions.

With the non-equivocal results it produced, this technique was probably one of the best ways to compare wetting conditions, as no subjective measurements were necessary. Unfortunately, its use was not possible for the present study. Firstly, it was very difficult to measure heat fluxes using this technique. The inclination of the substrate would cause

the droplet thickness to lose its uniformity and that might have had an influence on the acquired temperatures. Secondly, the objective of the project was to measure and compare heat fluxes for different wetting conditions. For non-wetting conditions, the droplets produced would simply fall off the substrate and for these droplets no temperature acquisition was possible. The comparison between the different wetting conditions would then not occur. In conclusion, this process would seem to be more adapted to dynamic wetting experiments where no thermal flux measurements are required.

3.3.3 – Spread factor

The last technique that was used in this project to evaluate dynamic wetting was the “spread factor”. This method is widely used in the field of plasma spraying, Amada et al. [22] and Ulrich et al. [21] are among the authors who have used it. This method is the simplest and easiest way to evaluate dynamic wetting. The spread factor is a measure of the flattening ratio of the droplet. One can find the spread factor (ξ) by simply dividing the final diameter of the droplet by the initial diameter.

$$\text{Spread factor} = \xi = \frac{d_f}{d_i}$$

The final diameter (d_f) is found once the droplet has completely spread on the surface, whereas the initial diameter (d_i) is measured just before the droplet touches the substrate (see Figure 3.6).

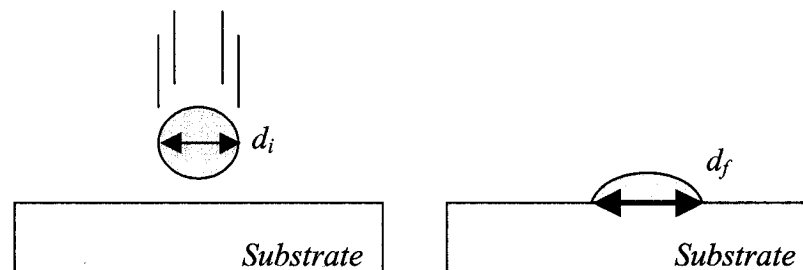


Figure 3.6 – Measure of the initial and final diameter to calculate the spread factor

With this method, dynamic wetting can be estimated very rapidly. Also, the calculated factors can be used easily for comparison with the larger spread factors identifying the

better wetting conditions. Ebrill [17] showed that spread factors were increasing as the contact angles were decreasing, showing the intrinsic relationship of the two.

3.4 – Heat Transfer

3.4.1 – One Dimensional Transient Heat Conduction Equation

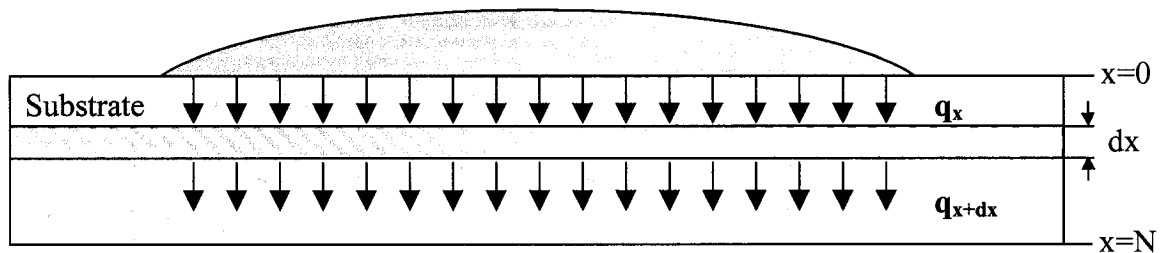


Figure 3.7 – One-dimensional heat conduction in a substrate

Now that the aspects of wetting and dynamic wetting have been covered in the previous sections, it is time to take a look at the heat transfer from the droplet to the substrate. There are three modes by which heat is exchanged with the surrounding environment, namely: radiation, convection and conduction. Due to the relatively low temperature of the aluminium droplets, radiation losses are very small compared to conduction. Also, airflow present around the droplets does not have a significant impact on the heat transfer and so, convection is not a major factor during solidification. Therefore, it is assumed that the energy released by the aluminium droplets is made mainly through conduction from the droplet to the substrate. The use of a copper substrate reinforces this assumption, since the copper substrate and its high thermal conductivity act as a powerful heat sink. Here, heat flow during the solidification of the droplets is assumed to be mainly one-dimensional in the first 5 millimetres of the substrate under the droplet, as illustrated in Figure 3.7. The same assumption was made by Todoroki et al. [40] using a similar set-up. Since this is a comparative study conclusions should not be affected by adopting this hypothesis.

When there is a temperature gradient in a solid, energy is transferred from the high-temperature region to the lower one. Heat is conducted through the solid and the heat transfer rate (q) per unit area (A) is equal to the gradient of temperature times proportionality constant called the thermal conductivity k . This yields the well known Fourier's law of heat conduction:

$$\frac{q}{A} = -k \frac{\partial T}{\partial x} . \quad (3.27)$$

When a droplet impinges on the copper substrate used in the experimental set-up, heat conduction is established in the substrate as shown in Figure 3.7. Performing a heat balance analysis on the small control volume of thickness dx (shaded in Figure 3.7), allows one to write the following:

Energy conducted into control volume's top surface + heat generated within the element =
change in internal energy + energy conducted out of control volume's bottom surface (3.28)

where,

$$\text{energy conducted in} = q_x = -kA \frac{\partial T}{\partial x} , \quad (3.29)$$

$$\text{heat generated within the element} = 0, \quad (3.30)$$

$$\text{change in internal energy} = \rho CA \frac{\partial T}{\partial t} dx \quad (3.31)$$

$$\text{energy conducted out} = q_{x+dx} = -kA \left. \frac{\partial T}{\partial x} \right|_{x+dx} = -A \left[k \frac{\partial T}{\partial x} + \frac{\partial}{\partial x} \left(k \frac{\partial T}{\partial x} \right) dx \right]. \quad (3.32)$$

In equation 3.31, C and ρ represent the specific heat ($\text{J/kg} \cdot ^\circ\text{C}$) and density of copper (kg/m^3) respectively. Making the appropriate substitutions in 3.28, we obtain the following relationship:

$$-kA \frac{\partial T}{\partial x} = \rho CA \frac{\partial T}{\partial t} dx - A \left[k \frac{\partial T}{\partial x} + \frac{\partial}{\partial x} \left(k \frac{\partial T}{\partial x} \right) dx \right], \quad (3.33)$$

or, dividing each term by $A dx$;

$$\frac{\partial}{\partial x} \left(k \frac{\partial T}{\partial x} \right) = \rho C \frac{\partial T}{\partial t} . \quad (3.34)$$

This partial differential equation describes transient one-dimensional heat-conduction and is termed Fourier's 2nd Law. The initial condition for the experiments is that the temperature within the thick copper block substrate at time $t=0$ is constant from the top to the bottom surface. The first boundary condition is found by stating that the temperature at $N = 5 \text{ mm}$ is equal to the temperature measured by the second thermocouple. The second boundary condition is that for times $t \geq 0$, a heat flux is applied at the surface of the substrate. Translated in mathematical language, these conditions are respectively given by:

$$T(x,0) = T_o \quad 0 \leq x \leq \infty \quad (3.35)$$

$$T(N,t) = T_{measured} \quad t \geq 0 \quad (3.36)$$

$$-k \left. \frac{\partial T}{\partial x} \right|_{x=0} = q(t) \quad t \geq 0. \quad (3.37)$$

For the present experiment, the expression for the thermophysical properties of copper C , k and ρ were the following [56, 60, 51]:

$$C = 4.77 \cdot 10^{-1} - 1.68 \cdot 10^{-4} T - 5.07 \cdot 10^{-3} T^{-2} + 1.49 \cdot 10^{-7} T^2 \quad (\text{kJ kg}^{-1} \text{ K}^{-1}) \quad (3.38)$$

$$k = 419 - 6 \cdot 10^{-2} T \quad (\text{W m}^{-1} \text{ K}^{-1}) \quad (3.39)$$

$$\rho = 8960 \quad (\text{kg m}^{-3}). \quad (3.40)$$

3.4.2 – Inverse Heat Conduction Problem Method

Using the transient one-dimensional heat conduction equation as a mathematical model for the temperature inside the substrate (equation 3.34), the objective of the heat transfer study is to find the heat flux at the surface of the substrate ($x = 0$) given by the boundary equation (3.37). In classical problems, the boundary conditions are known and used to determine the temperature profile in the substrate. Here, the boundary condition at the substrate surface is unknown and is calculated using the temperatures measured in the substrate; this is called the inverse heat conduction problem. In this study, the technique and software code used to calculate heat fluxes entering the substrate was the same as the

one employed by Bouchard et al. [34]. This technique is based on the sequential function-specification method proposed by Beck [27], and only a brief description is given here.

The contact time between the droplet and the substrate was divided into m individual intervals. The heat flux was considered to be constant within each interval, but to vary from one to another. The heat flux was found using a nonlinear estimation procedure, minimizing the sum of squares function (S) with respect to some functions approximating the heat flux in each interval m at the substrate surface $q(x = 0, t)$:

$$S = \sum_{i=1}^r \sum_{j=1}^J (Y_{j,m+i-1} - T_{j,m+i-1})^2 \quad (3.41)$$

where $Y_{j,m+i-1}$ is the measured temperature at the time interval $m+i-1$ and $T_{j,m+i-1}$ is the calculated temperature using an explicit finite-difference technique (see table 3.3). The subscript r and J refer respectively to the number of future time steps and the number of thermocouple inserted inside the substrate (two in this study). The number of future time steps is a parameter used to increase the stability of the iterative process; it was usually equal to 3 or 4 in the present study. Making temporarily the assumption that all subsequent heat fluxes are equal,

$$q_{m+2} = q_{m+3} = \dots = q_{m+r} = q_{m+1} \quad (3.42)$$

one can determine the value of $T_{j,m+i-1}$ using the n^{th} iteration of the Taylor series approximation:

$$T_{j,m+i-1}^n \approx T_{j,m+i-1}^{n-1} + \frac{\partial T_{j,m+i-1}^{n-1}}{\partial q_m^n} (q_m^n - q_m^{n-1}), \quad (3.43)$$

where,

$$\frac{\partial T_{j,m+i-1}^{n-1}}{\partial q_m^n} = Z_{j,m+i-1}^{n-1} \approx \frac{T_{m+i-1,j}^{n-1}(q_m^{n-1}(1+\delta)) - T_{m+i-1,j}^{n-1}(q_m^{n-1})}{\delta q_m^{n-1}} \quad (3.44)$$

and the fixed value increment δ for q_m^{n-1} was chosen to be 0.001. Introducing equations 3.43 and 3.44 in 3.41 one obtain,

$$S = \sum_{i=1}^r \sum_{j=1}^J (Y_{j,m+i-1} - T_{j,m+i-1} - Z_{j,m+i-1}^{n-1} \cdot (q_m^n - q_m^{n-1}))^2. \quad (3.45)$$

The sum of square function will be at a minimum if $\frac{\partial S}{\partial q_m^n} = 0$, therefore we obtain:

$$\frac{\partial S}{\partial q_m^n} = 0 = \sum_{i=1}^r \sum_{j=1}^J (T_{j,m+i-1} \cdot Z_{j,m+i-1}^{n-1} - Y_{j,m+i-1} \cdot Z_{j,m+i-1}^{n-1} + (Z_{j,m+i-1}^{n-1})^2 \cdot (q_m^n - q_m^{n-1}))$$

or

$$q_m^n = q_m^{n-1} + \frac{\sum_{i=1}^r \sum_{j=1}^J (Y_{j,m+i-1} - T_{j,m+i-1}) \cdot Z_{j,m+i-1}^{n-1}}{\sum_{i=1}^r \sum_{j=1}^J (Z_{j,m+i-1}^{n-1})^2}. \quad (3.46)$$

Using successively and in loop this expression and the explicit finite difference temperature approximations shown in the table below, allows one to find the solution iteratively for the heat flux acting at the substrate surface for each time interval m . Iterations begin with an initial value for q_m^n , and are performed until the following condition is met:

$$\frac{q_m^{n+1} - q_m^n}{q_m^n} \leq 0.005. \quad (3.47)$$

Table 3.3 – Explicit Finite Difference Temperature Approximations Obtained from Equation 3.34 [57]

Node	Substrate Temperature
1	$T_1^{p+1} = T_1^p + \frac{2k_1^p \Delta t}{\rho C_1^p \Delta x^2} \left[(T_2^p - T_1^p) + \frac{q^p \Delta x}{k_1^p} \right] + \frac{dk}{dT} \frac{\Delta t}{\rho C_1^p} \left(\frac{q^p}{k_1^p} \right)^2$
i	$T_i^{p+1} = T_i^p + \frac{k_i^p \Delta t}{\rho C_i^p \Delta x^2} \left[(T_{i+1}^p - 2T_i^p + T_{i-1}^p) + \frac{dk}{dT} \frac{1}{4k_i^p} (T_{i+1}^p - T_{i-1}^p)^2 \right]$
N	$T_N^p = T_{Measured}^p$

4. EXPERIMENTAL PROCEDURES

4.1 – Procedures

This section describes the experimental procedures used for this work. Detailed description of the set-up is given in section 4.2. The experimental set-up constructed for the present work is similar to the one of Ebrill et al. [17, 24-26] and Todoroki et al. [39-41]. Figure 4.1 is a depiction of the apparatus. It consisted of a copper substrate, a graphite crucible with a small hole at the bottom, a spindle made of graphite, a resistance-heating element, an electric motor, a moving table and a high-speed camera.

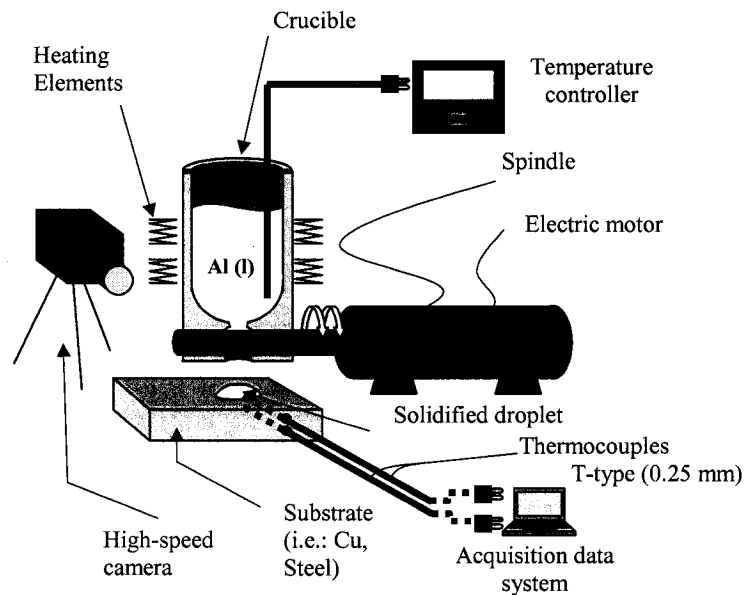


Figure 4.1 – Experimental Set-Up for the Simultaneous Characterization of Dynamic Wetting and Heat Transfer at the Initiation of Solidification of Aluminium.

Typically, 200 grams of aluminium were melted and held at 725 °C in the graphite crucible using electrical resistance heating elements. An electric motor was used to rotate the spindle in which a dimpled cavity was machined. As it faced the small hole at the bottom end of the crucible, this cavity was filled with liquid aluminium and a molten droplet was formed following the rotation of the spindle. Then, the droplet was released under free-fall conditions, impinged on the copper-substrate, and solidified. Two T-type

thermocouples (0.25 mm) were inserted in the centre of the substrate. These thermocouples measured the evolution of temperature at a frequency of 1000 Hz. Finally, the high-speed camera captured the evolution in the shape of the droplet as it spread on the substrate. The images taken by the camera were analysed simultaneously with the data acquired for heat transfer. With this set-up it was possible to vary various experimental conditions such as the chemical composition of the alloy, the volume of the droplet, the height of fall, the substrate temperature, its surface condition, the composition of the gas, etc... The following section gives a description of the components that were used in the set-up, along with some pictures.

4.2 – Description of experimental set-up

Of foremost importance was to determine the material used to build the spindle and the crucible in which the aluminium was melted. Graphite was chosen for its non-wetting and non-reacting properties towards aluminium, as well as for its good machinability. The spindle (75 mm long, 25 mm in diameter) was tightly fitted into the bottom of the crucible (155 mm high, 75 mm in diameter). This can be seen in Figure 4.2. After five experiments, graphite was found to deteriorate and became porous at temperatures used to melt the aluminium. The friction that would necessarily occur between the crucible and the spindle during its rotation produced a small amount of graphite dust, which would fall on the substrate prior to the impingement of the droplets. Since this graphite dust could have an impact on wetting and/or heat transfer, the decision was taken to select another material to build the spindle. Many possibilities were considered and tested; spindle made of alumina, boron nitride, stainless steel, steel with a high percentage of tungsten, and steel coated with tungsten. In every case, except for boron nitride, the graphite dust problem was eliminated, but the droplet of molten aluminium stuck to the surface of the material and the droplets hardly fell, if even forming. A tungsten coated steel spindle gave the best performance for droplet formation, but the coating started to oxidize after three experiments and chemical reactions with aluminium compromised its use. Another obstacle raised by the use of steel spindles was that the thermal expansion of the spindles at 725°C was too large compared to the graphite crucible and it was sometimes

impossible to bring it into rotation. After many fruitless trials, it was decided to perform all the experiments with crucibles and spindles made of graphite. To avoid the deposits of dust on the substrate, each spindle was employed no more than three times and crucibles were replaced after six experiments. Furthermore, a clean piece of tissue was used to wipe the substrate after each test. The good machinability of graphite proved useful in these tests since grooves and dimple were to be carved on each spindle. The grooves were machined in order to screw the spindle on the steel rod connected to the electric motor and the dimple was made to allow the droplet formation. The size of the dimple depended on the desired volume of droplet to be produced. Dimple volumes varied from 0.1 cm^3 to 0.9 cm^3 , which allowed generating droplets of 0.25 grams to 2 grams. It is important to point out that the temperature acquisition was easier for bigger droplets, but inertial effects (Weber number) were also increased and a compromise had to be found to ensure good temperature and dynamic wetting measurements. Most of the results presented here were obtained with droplets mass from 0.3 grams to 0.75 grams. Two aluminium alloys were used during the experimental study: AA1070 (pure aluminium) and AA5754 (3.41wt% Mg, 0.14 Mn, 0.07 Si, 0.18 Fe, 0.015 Ti, 0.009 V, 0.004 Cu).

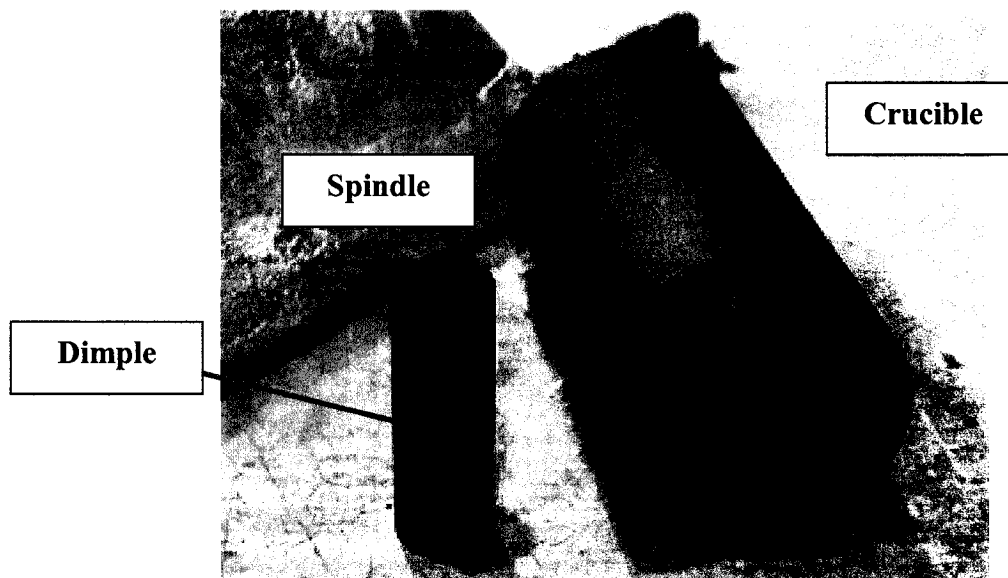


Figure 4.2 – Picture of the graphite crucible and spindle

The droplet volumes were not the only parameter that could vary in the experiments. As stated earlier, the set-up was built in order to study a wide variety of parameters, since any transformation was an easy task. For instance, the moving table on which the electric motor and crucible lay could be displaced in the x, y and z directions, allowing experiments to be carried out for different heights and positions.

Moreover, the whole set-up was enclosed in an aluminium chamber to provide a controlled atmosphere (see Figure 4.3). A Plexiglas window was covering the front of the chamber so that it was possible to look inside and to take pictures with the high-speed camera. A gauntlet was also used to manipulate the set-up inside the chamber when a controlled atmosphere was used. Air, argon and helium were employed and their influence on the heat transfer and dynamic wetting were analysed. The chamber was not perfectly gastight, but it was possible to decrease the amount of oxygen to fairly low concentrations. A gas analyser linked to the chamber recorded an oxygen concentration of 0.2% in a helium atmosphere and 0.02% in argon. The objective was not necessarily to obtain super-pure atmosphere since the industrial twin-roll caster process does not reach such conditions.

Another item that was interchangeable is the metallic substrate. The substrate was maintained in a vice, making it easy to replace it. For this project, only copper substrates were used, but any type of block would fit in. Figure 4.4 shows a typical substrate employed for the experimental study. The substrates (50 mm x 120 mm x 20 mm) were made of electrolytic tough pitched, ETP, copper with a purity of 99.9+ percent. A section of the substrates (50 mm x 65 mm x 7 mm) was removed so that it would be easier to take images with the high-speed camera. Normally experiments were performed at ambient temperature, but it was possible to cool or heat the substrate, using water-cooled or heated blocks, respectively.

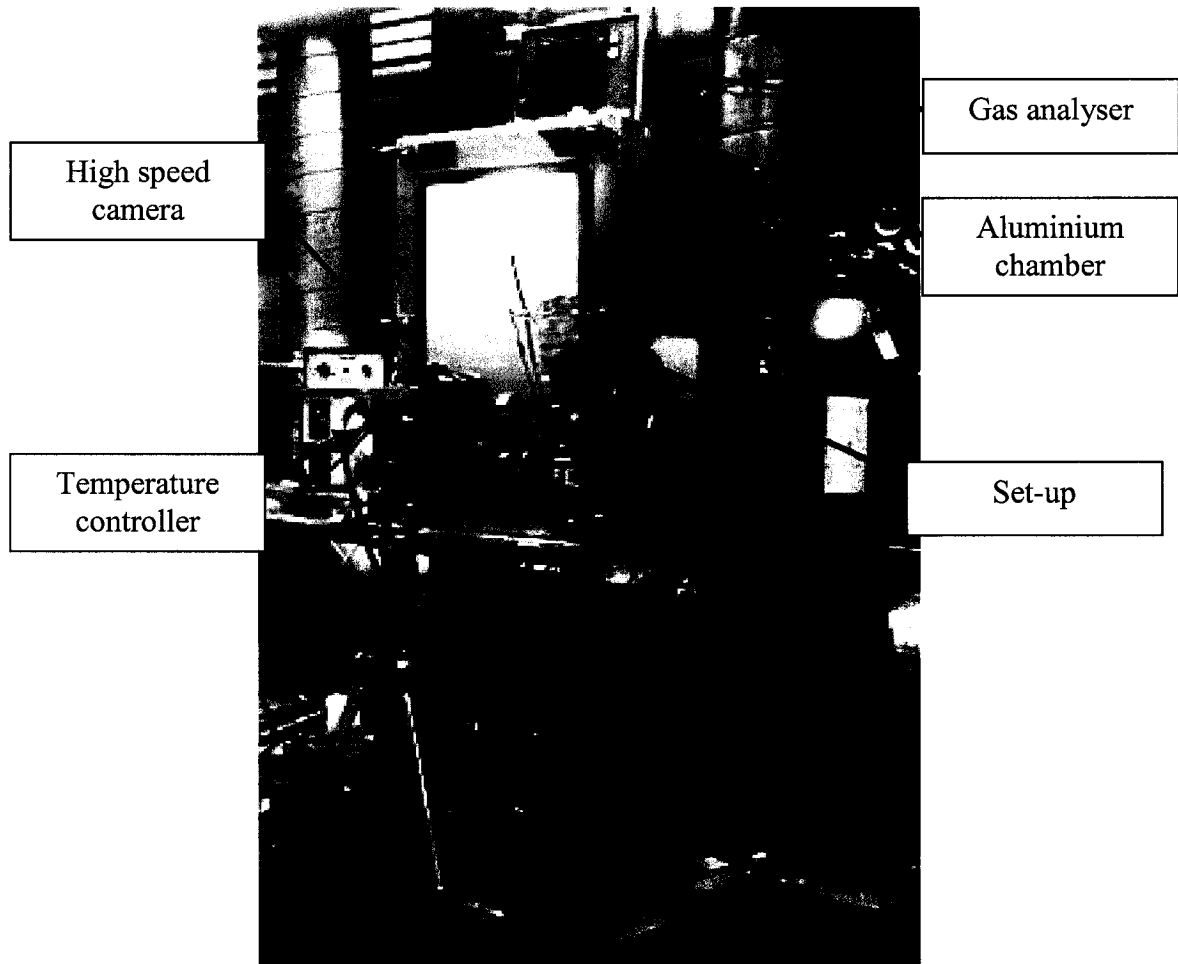


Figure 4.3 – Picture of the set-up with the aluminium chamber

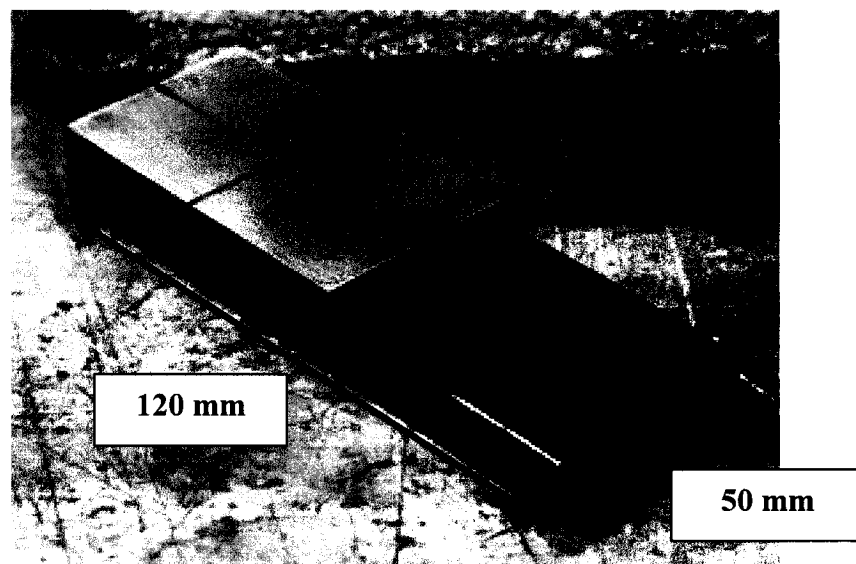


Figure 4.4 – Picture of the polished copper substrate used in the experimental set-up

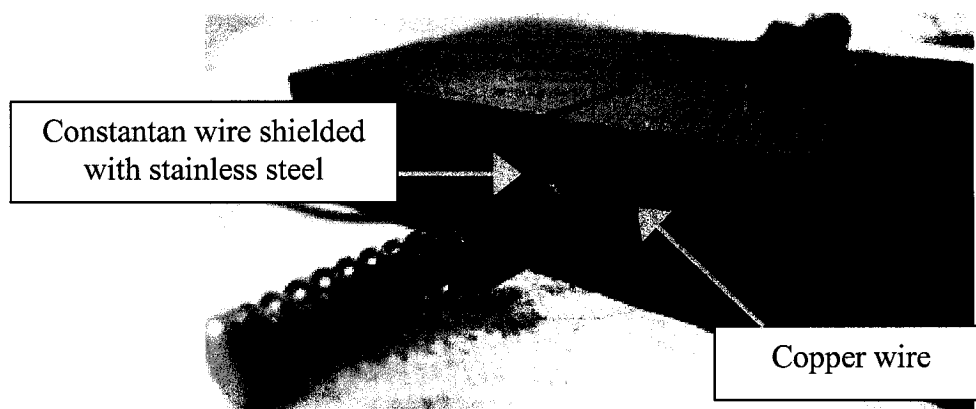


Figure 4.5 – Side view of a sand-blasted copper substrate showing the constantan wire inserted inside the substrate and the copper wire completing the thermocouple circuit. The thermocouple's holes are normal to the side surface of the substrate.

Two substrates were used for the experiments, a polished one having an average surface roughness (R_a) of $0.2\ \mu\text{m}$ and another one that had been sand-blasted to produce an average surface roughness (R_a) of $6.4\ \mu\text{m}$. Both substrates had two T-type thermocouples ($0.25\ \text{mm}$) inserted into drilled holes, one about $1\ \text{mm}$ below the surface, and the other at about $5\ \text{mm}$. Table 4.1 shows the exact depth of the thermocouples for both substrates. The diameter of the holes was $1\ \text{mm}$ ($0.038\ \text{inch}$). The thermocouple arrangement was semi-intrinsic where the substrate itself acts as one thermocouple element [42] (see Figure 4.5). T-type thermocouples are made of strands of constantan and copper. The constantan wire was shielded with a stainless steel sleeve containing a ceramic insulator; it was pushed and held in contact with the bottom of the drilled hole using a spring. The drilled hole reached the mid width of the substrate. The copper wire was screwed on the copper substrate and completed the electrical circuit. Therefore, no welds were necessary at the hot junction of the thermocouples; this provided a faster response as the temperature readings were carried out at a frequency of $1000\ \text{hertz}$.

The quality of the temperature measurements is not the only factor to ensure acceptable heat flux results. Lines were drawn on the substrates to indicate the thermocouple locations inside it. In this way, it was much easier to determine if the falling droplets were impinging at the right position and it also ensured that the heat fluxes obtained were

representative. Any droplet not falling precisely over the thermocouple locations was ignored in the analysis.

Table 4.1 – Position on the thermocouples inside the two substrates

Substrate	Thermocouple #1	Thermocouple #2
<i>Polished</i>	0.69 mm	4.85 mm
<i>Sand Blasted</i>	0.98 mm	4.90 mm

Finally, a high-speed camera was used to study the evolution of the droplet morphology during its impingement on the copper substrate. The camera could record images up to 10 000 frames per second, but normally the operating speed was 1000 frames per second, thus ensuring a better image quality. The camera memory could record up to a maximum of 8000 frames and these were converted into .avi files. The images taken were analysed simultaneously with the heat fluxes calculated from the acquisitioned temperatures. Both the high-speed camera and the data acquisition system were started at the same time using a unique controller for the two.

5. RESULTS AND DISCUSSION

Different experimental conditions were investigated during the tests, but only one parameter was varied at the time. The experimental procedures were aimed at providing a comparative study between the different conditions. The conditions were chosen to produce differences in the wetting, in order to verify how heat transfer was affected.

The role of gaseous atmosphere, the initial temperature of the substrate, the surface condition of the substrate and the composition of the aluminium alloy were investigated. Within each experiment, all, but the parameter to be studied, were kept constant. The initial temperature of the aluminium was fixed for all experiments at 725°C and the heights of fall for the droplets were chosen to be 5 and 10 millimetres. The results presented here are average values for a minimum of five trials (droplets). When a droplet fell outside the specified impact point target (see section 4.2), the associated heat flux was ignored. The reproducibility of the results was excellent since all the heat flux curves were within 10 to 15% of the calculated average. The first section of this chapter gives an overview of the results obtained during the experiments. The results for the above mentioned parameters are presented in the following sections.

5.1 – Overview of results obtained

As seen in the chapter 4, two data acquisition systems were used in performing the experiments, one for the high-speed camera and the other one for the thermocouples. The most important characteristic for the two systems was to produce results with good resolution at a very high frequency (500 data per second and more).

In the case of the high-speed camera, these conditions were easily met. The camera could record up to 10 000 frames per second, but a rate of 1000 images per second was easily sufficient for this set of experiments. Figure 5.1 illustrates an example of the interaction of the droplet with the substrate as taken by the high-speed camera. The droplet first impacted and then spread out on the substrate. As solidification proceeded, liquid metal in

the droplet was constantly moving and the top surface was oscillating. Solidification was completed after approximately 0.4 seconds for the droplet shown.

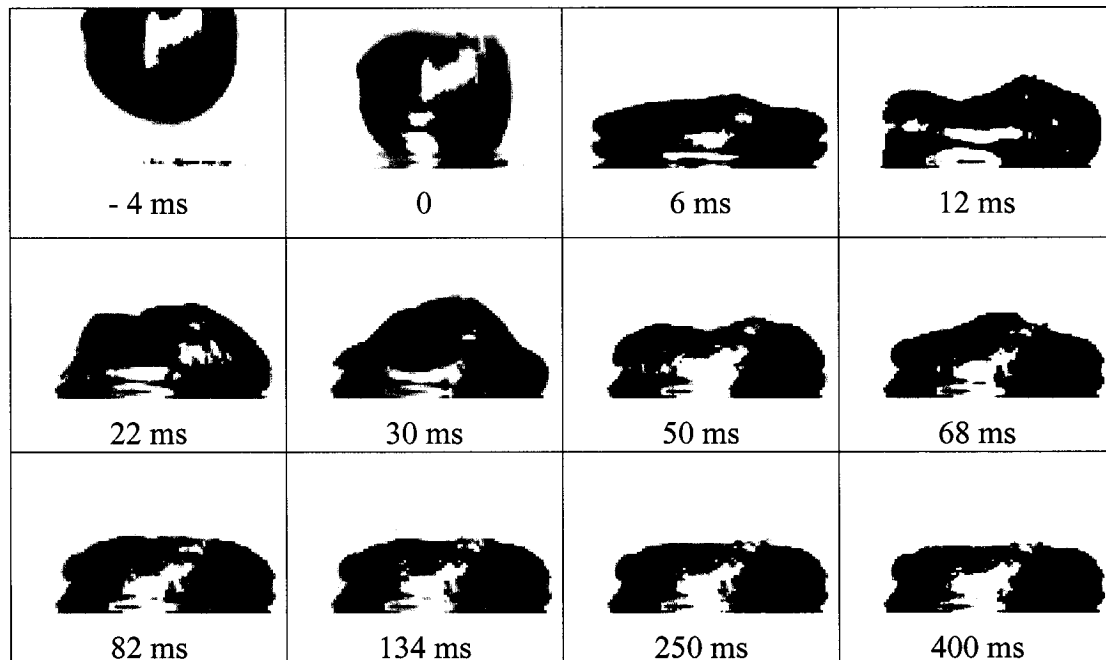


Figure 5.1 – Droplet Impinging on a Substrate Surface (0.42 g, height of fall = 10mm)

A very good resolution in the temperature measurements was also obtained with the semi-intrinsic method. An example of the temperatures read by the thermocouples inserted in the substrate is shown in Figure 5.2. The one at 1 mm below the substrate was always more sensitive than the other at 5 mm. As shown in Figure 5.2, there was a time interval of 30 milliseconds between the rise in temperature read by the thermocouple at 1 mm and the one at 5 mm. The temperature started rising at 1.095 seconds for the first thermocouple and at 1.125 seconds for the second one.

A sensitivity analysis using the IHCP model showed that it was important to determine precisely the position of the two thermocouples. Future time steps were also kept as low as possible in the model. Other parameters were analysed in previous works by Bouchard et al. [33, 34].

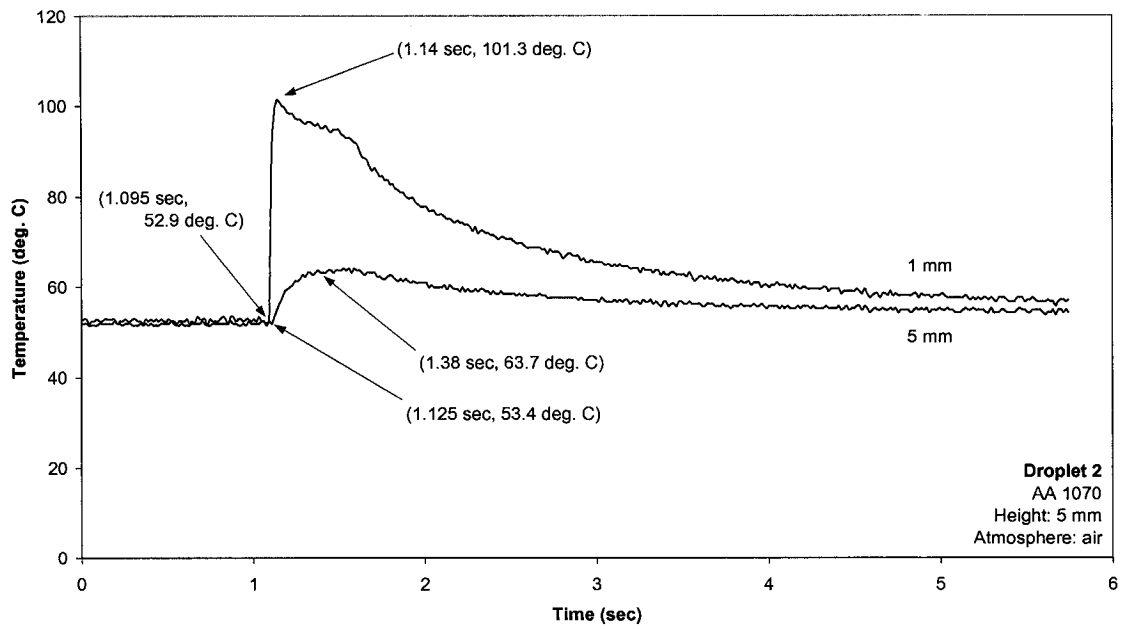


Figure 5.2 – Temperature Profiles in the Substrate for a Droplet Falling from a Height of 5 mm

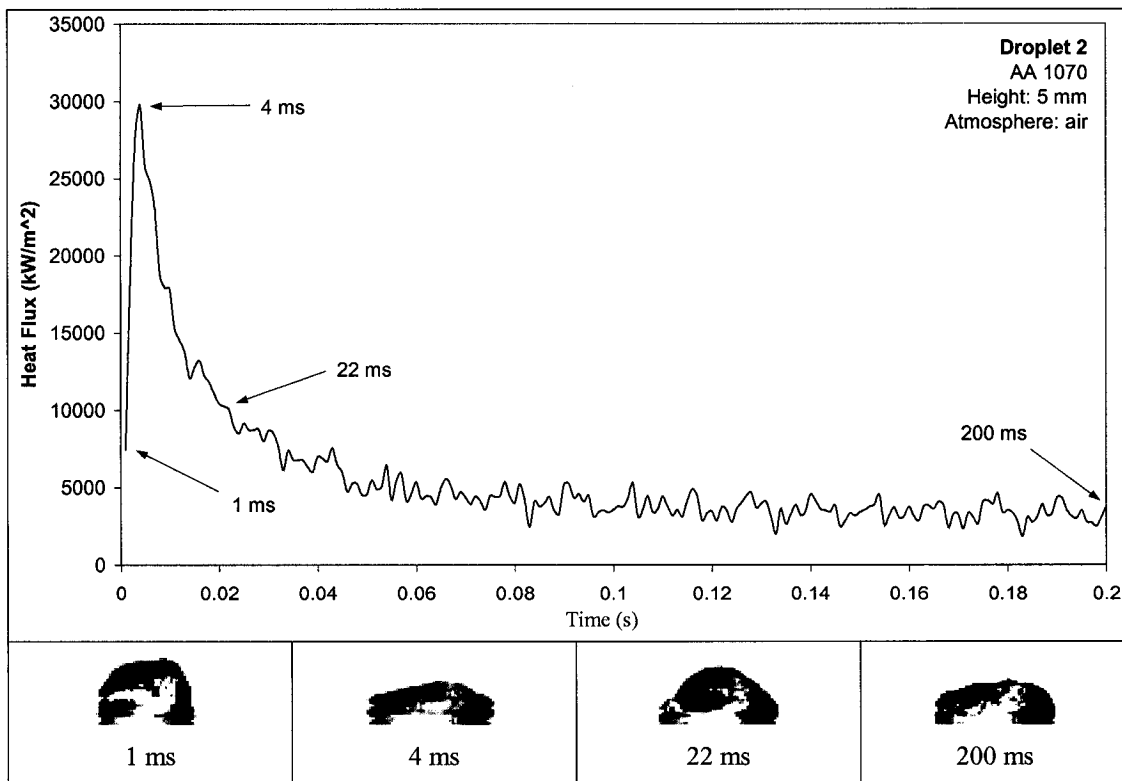


Figure 5.3 – Heat Flux as a Function of Time and Sequence of the Droplet Impinging, Wetting and Spreading at Specific Times for a Height of Fall of 5 mm

This temperature evolution was then used to calculate the heat flux curves. Figure 5.3 shows the heat flux evolution and the concurrent shape of the droplet at specific times. It is considered that the correspondence between the heat flux and the shape of the droplet is within ± 2 milliseconds.

Finally, all the heat flux curves obtained for a unique condition were assembled on one graph as shown on Figure 5.4 and an average curve was found for comparison purposes with other experimental conditions.

The results illustrated in Figure 5.1 to 5.4 are typical of those obtained with the experimental set-up. The following sections give detailed results for the four parameters studied. Each section is introduced by giving the conditions under which the tests were performed, followed by the experimental results and discussions.

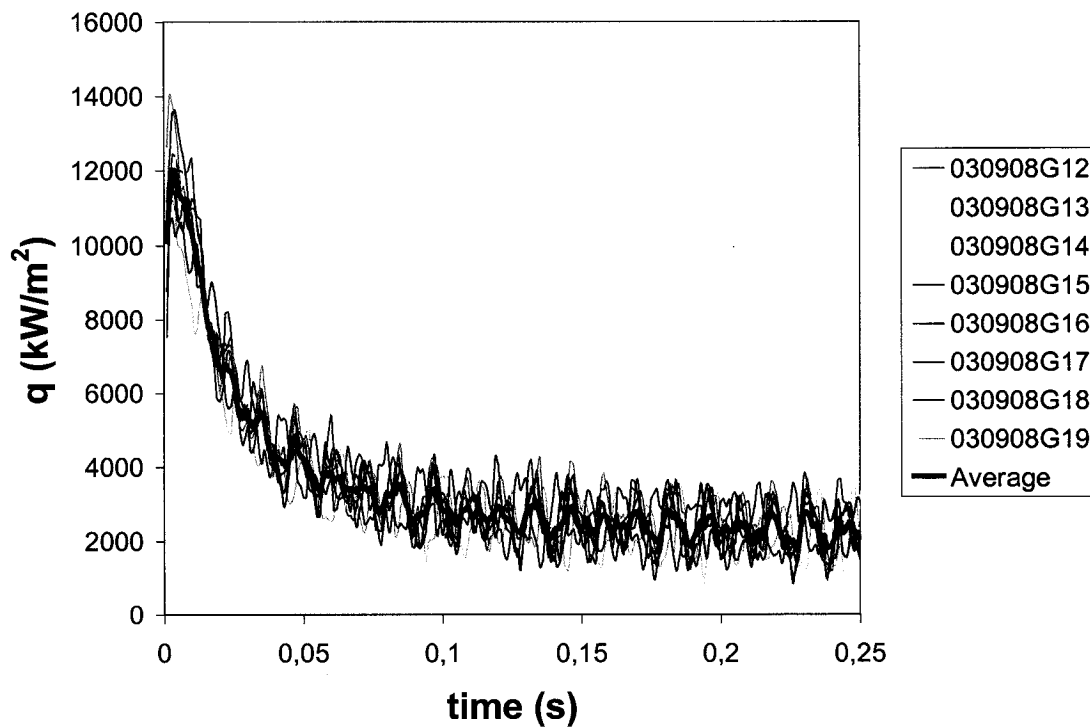


Figure 5.4 – Heat flux curves and the calculated average obtained for a set of droplets (AA1070, air, height of fall = 10 mm, 0.34 grams, avg. spread factor = 1.19)

5.2 – Role of alloy composition of droplets on heat transfer and dynamic wetting

Table 5.1 – Experimental conditions for determining the role of alloy composition on heat transfer and dynamic wetting

	AA1070	AA5754
<i>Alloy studied</i>	AA1070 (99.7% Al)	AA5754 (3.41% Mg)
<i>Atmosphere</i>	Air	Air
<i>Substrate surface condition</i>	Polished	Polished
<i>Initial temperature of the substrate</i>	room temp.	room temp.
<i>Weight of the droplets</i>	0.47 g	0.47 g
<i>Weber number (We)</i>	3.7	3.7

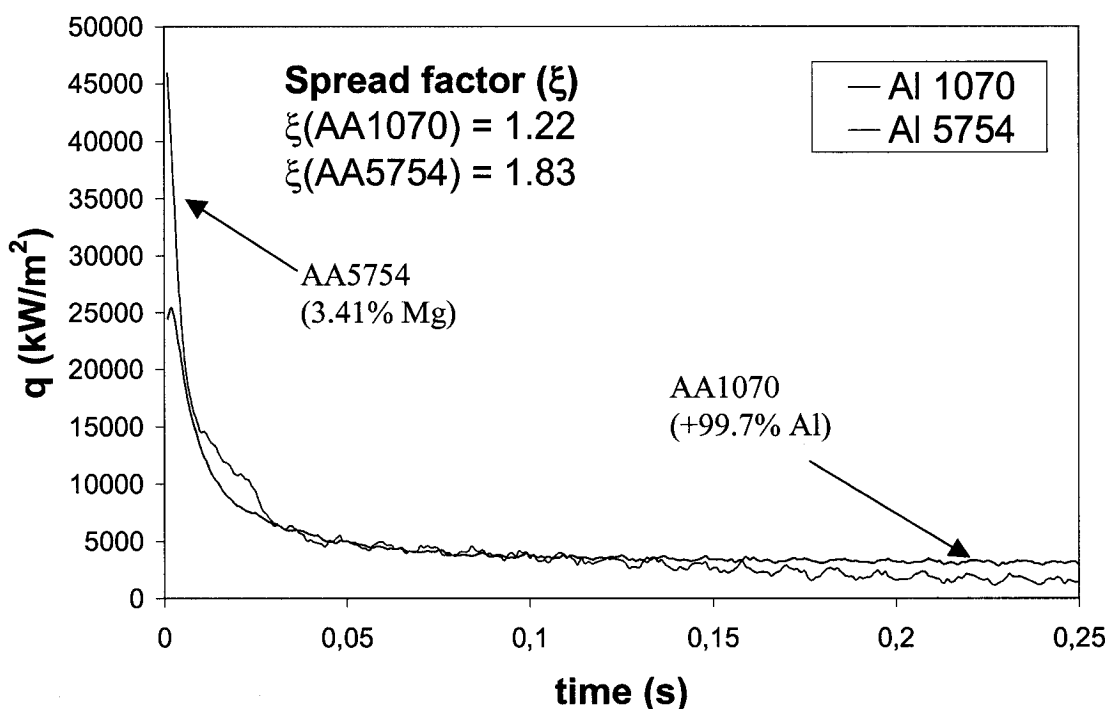


Figure 5.5 – Effect of magnesium content in aluminium on heat transfer and dynamic wetting

This experiment was performed to study the influence of alloying elements on heat transfer and dynamic wetting. Two aluminium alloys were studied, namely, AA1070 and AA5754. The first one was aluminium of commercial purity (+99.7 % Al) and droplet

formation was accompanied by the creation of an aluminium oxide layer on the droplet surface. For AA5754, the aluminium alloys contained 3.41 wt.% magnesium.

The significant difference in the dynamic wetting characterized by the spreading factor (1.22 for AA1070 vs. 1.83 for AA5754) shows that the better wetting of the AA5754 alloy was accompanied by a large initial heat flux (see Figure 5.5). This is observed between $t=0$ and $t=40$ milliseconds, the spread factor of AA5754 was much higher than for AA1070 and the peak heat flux for the AA5754 was almost twice the one of AA1070. It is important to notice that the spreading of a droplet after the initial contact with the substrate generally took three to ten milliseconds to be fully established after which, it remained constant. Therefore, the correspondence between these factors and heat fluxes is best determined during that period.

A second phase (40 milliseconds to 125 milliseconds) can be observed in the heat flux curve of Figure 5.5. During this phase, the heat fluxes between the two alloys are nearly the same. A third and final phase is also observed at $t>125$ ms where the heat flux for the AA5754 alloy is lower than the AA1070. This could be accounted by a larger contraction in the AA5754 droplet, and hence greater interfacial gap. Loulou et al. [42, 43] have also used a similar argument to explain a lower heat transfer in the later stages of solidification for their alloys.

According to the Ellingham diagram (see Figure 5.6) magnesium oxide forms at lower oxygen potentials than aluminium oxide in the temperature range studied; therefore the droplets were probably covered with an oxide layer of different chemical composition than those from aluminium of commercial purity. This had an impact upon the wetting of the droplets, since the spread factor was not the same for both alloys. Lang [49] showed that alloying aluminium with magnesium would decrease the surface tension of the aluminium by acting as a surface-active element.

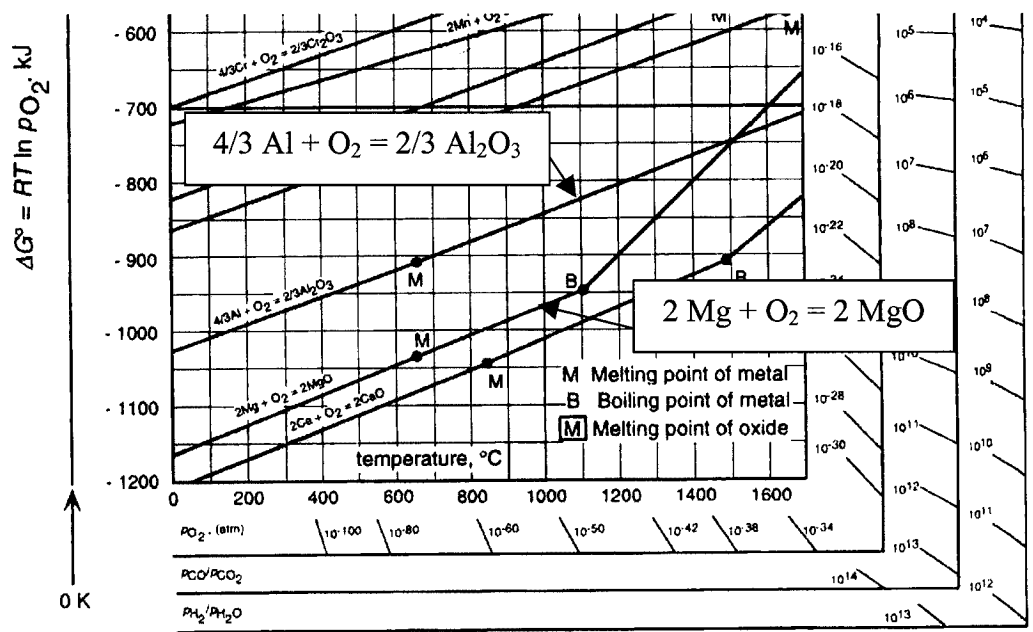


Figure 5.6 – Ellingham diagram for aluminium and magnesium oxides [52]

The important observation that can be made from the results obtained by increasing the magnesium content of aluminium is that a greater spreading of the droplet on the substrate provided a greater heat transfer at the initiation of solidification.

5.3 – Role of the initial temperature of the substrate on heat transfer and dynamic wetting

Table 5.2 – Experimental conditions for determining the role of initial temperature of the substrate on heat transfer and dynamic wetting

	80°C	175°C	275°C
<i>Alloy studied</i>	AA1070	AA1070	AA1070
<i>Atmosphere</i>	Air	Air	Air
<i>Substrate surface condition</i>	Polished	Polished	Polished
<i>Initial temperature of the substrate</i>	80°C	175°C	275°C
<i>Weight of the droplets</i>	0.37g	0.37g	0.37g
<i>Weber number (We)</i>	3.42	3.42	3.42

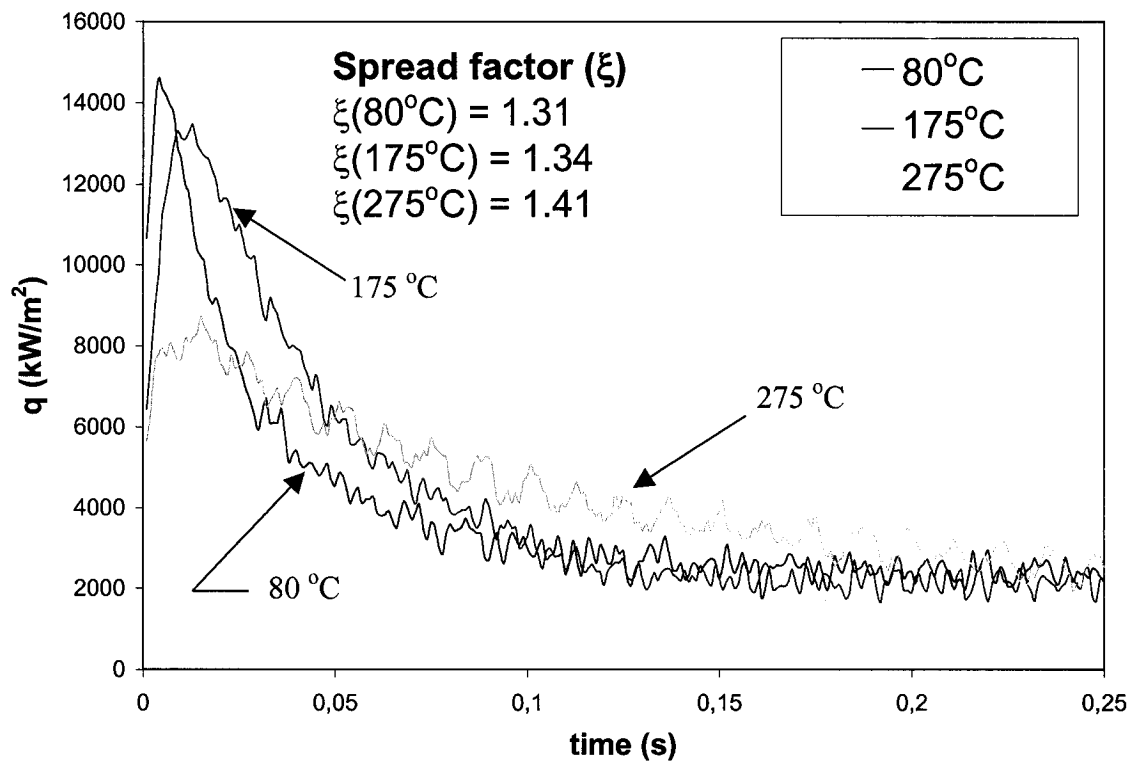


Figure 5.7 – Role of initial temperature of the substrate on heat transfer and dynamic wetting

The objective of this experiment was to determine if initial temperature of the substrate had an influence on heat transfer and dynamic wetting. The results for three different

initial substrate temperatures are shown in Figure 5.7. A significant oxidation at the surface of the substrate and sticking of the droplet was observed at 275°C but not at the lower temperatures. A different regime appears to have taken place at 275°C and consequently the results are discussed separately.

The peak value in the heat flux was slightly higher at 80°C than at 175°C but the overall heat that was transferred during the first 25 ms was higher at 175°C. The area under the curves yielding the total energy transferred during that period assesses this. This energy was greater at 175°C than at 80°C and the spread factor was accordingly larger at 175°C.

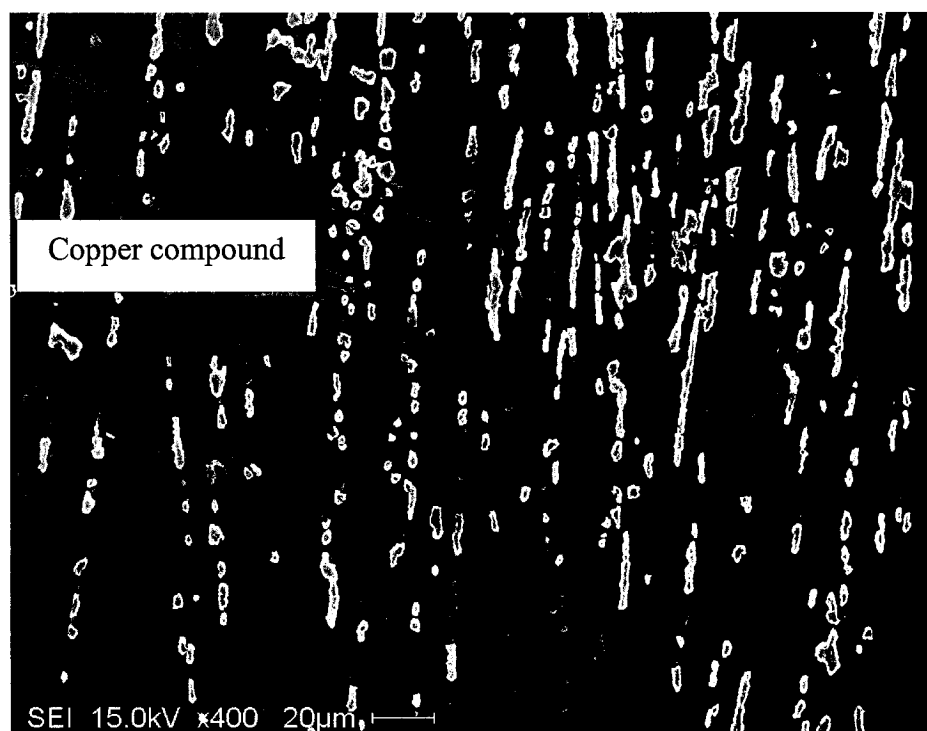
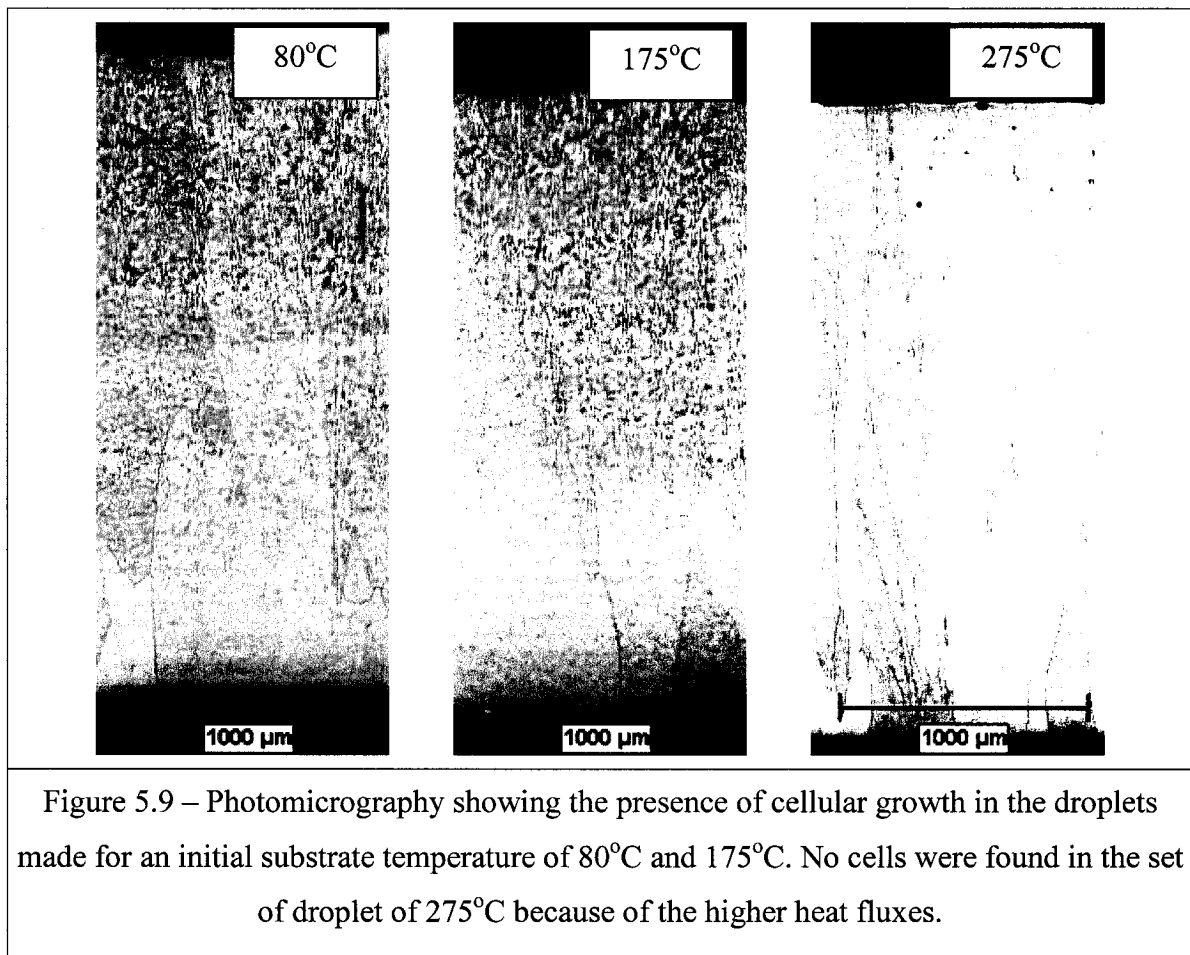


Figure 5.8 – Presence of copper compound, presumably an oxide, on the droplet surface in contact with the substrate

At a temperature of 275°C, the surface of the substrate became dark. This was associated to the formation of a thicker oxide layer than that observed at $T < 175^\circ\text{C}$. Below 175°C, the surface of the substrate retained its typical copper lustre. Sticking of the droplets was observed at 275°C and a reaction with the substrate appears to have taken place. This is

shown in Figure 5.8 where traces of the copper substrate appear at the surface of the droplet. This reaction only occurred at this temperature and not at the lower ones.

It is interesting to note from Figure 5.7 that after 25 ms the heat flux at 275°C was larger than that obtained at 80°C. The heat flux at 275°C is also larger than that at 175°C but after 50 ms. Sticking of the droplet may have taken place after solidification was initialized and this could explain that the heat flux at 275°C took 25 to 50 ms to become larger than that found at 80°C and 175°C.



The results of the microstructural analysis that was performed on droplets that solidified at the three substrate temperatures are shown in Figures 5.9 and 5.10. It is seen that the cellular structure is finer at 275°C than the other two temperatures. This indicates that the cooling rate was larger at this temperature. As mentioned earlier, the heat transfer at the

onset of solidification for the droplet solidifying on the substrate at 275°C was lower than at 80°C and 175°C, but this was reversed after a period of 25 to 50 ms. During that period, only the outside layer of the droplet would be solid while the inside would still go through the solidification process.

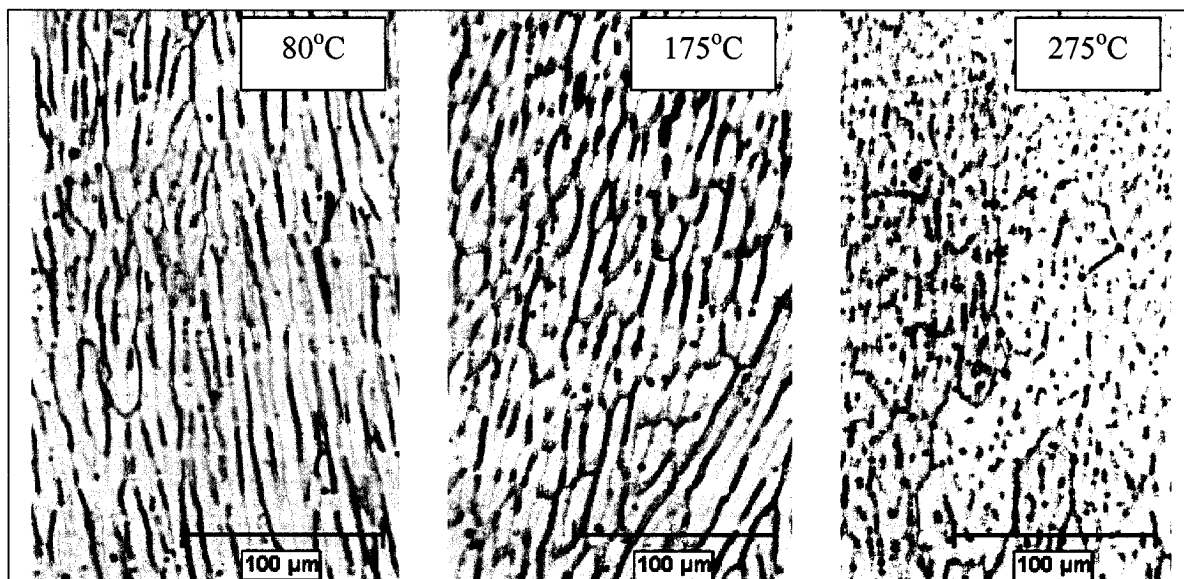


Figure 5.10 – Photomicrographs showing the size of the cells in the droplet structures for initial temperature of the substrate of 80°C, 175°C and 275°C. Based on these pictures, it is concluded that the cooling rate was larger at 275°C.

Therefore, looking at the evidence from Figures 5.8 to 5.10, it was clear that the heat flux and the dynamic wetting increased with initial substrate temperature as such, the improved wetting was again associated with improved heat fluxes.

5.4 – Role of the substrate surface condition on heat transfer and dynamic wetting

Table 5.3 – Experimental conditions for determining the role of the substrate surface condition on heat transfer and dynamic wetting

	<i>Polished</i>	<i>Sand blasted</i>
<i>Alloy studied</i>	AA1070	AA1070
<i>Atmosphere</i>	Air	Air
<i>Substrate roughness (Ra)</i>	0.2 μm	6.4 μm
<i>Initial temperature of the substrate</i>	27°C	27°C
<i>Weight of the droplets</i>	0.49 g	0.49 g
<i>Weber number (We)</i>	3.8	3.8

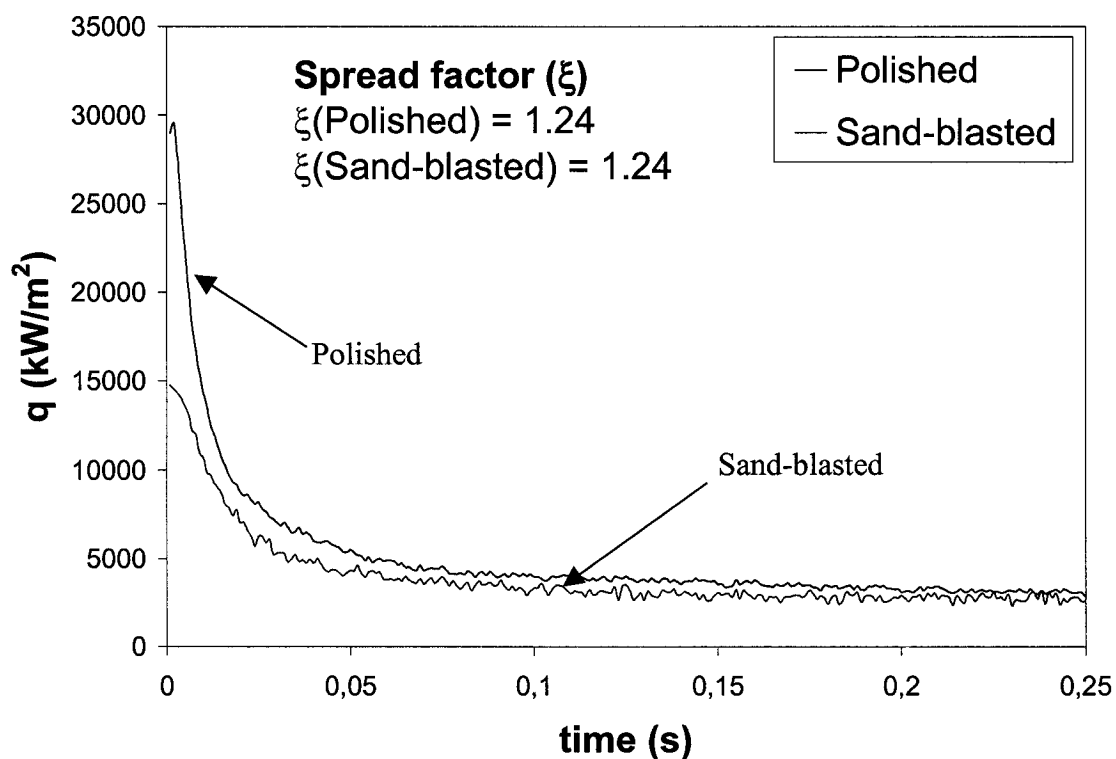


Figure 5.11 – Role of the substrate surface condition on heat transfer and dynamic wetting

The objective of this experiment was to study the effect of the substrate surface roughness over the dynamic wetting and the heat transfer during the solidification of AA1070

aluminium droplets. Two substrates were used; the first one was polished to obtain an average surface roughness (Ra) of 0.2 μm . The other was sand-blasted to produce an average surface roughness (Ra) of 6.4 μm . The results are shown in Figure 5.11. It is seen that increasing the surface roughness decreased the heat flux but did not have a sensible effect on the wetting as characterized by the spread factor.

Examination of the solidified droplets with a scanning electron microscope (SEM) provided an explanation for the lower heat fluxes. From the pictures given in Figures 5.12 to 5.14, it was observed that the surface area available for heat transfer was greater when the aluminium solidified on a polished surface compared to a rough one. In the latter, the aluminium only infiltrated the asperities near the impingement point and there was a poor contact of the droplet with the substrate as the droplet spread beyond impingement. This is illustrated by the sketch in Figure 5.15, which was drawn from information given by the SEM examination. Authors have shown that the heat flux was affected by the surface condition of the substrate. Muojekwu et al. [48] for instance have demonstrated, using a different set-up, that for aluminium alloys, the heat flux was lowered with an increase in the roughness of the substrate.

The SEM examination also provided an explanation to the equivalence in the spread factors for the two substrates. The surface condition of the droplets being very much the same, except near the impingement point, indicates that the spreading occurred very similarly in both substrates and was not hindered by the asperities of the rougher one. Here, the gas phase trapped in the asperities may have played the role of a cushion on which the droplet spread. There will be more research necessary to validate this explanation, for example by increasing the roughness, since beyond a certain point asperities should hinder spreading.

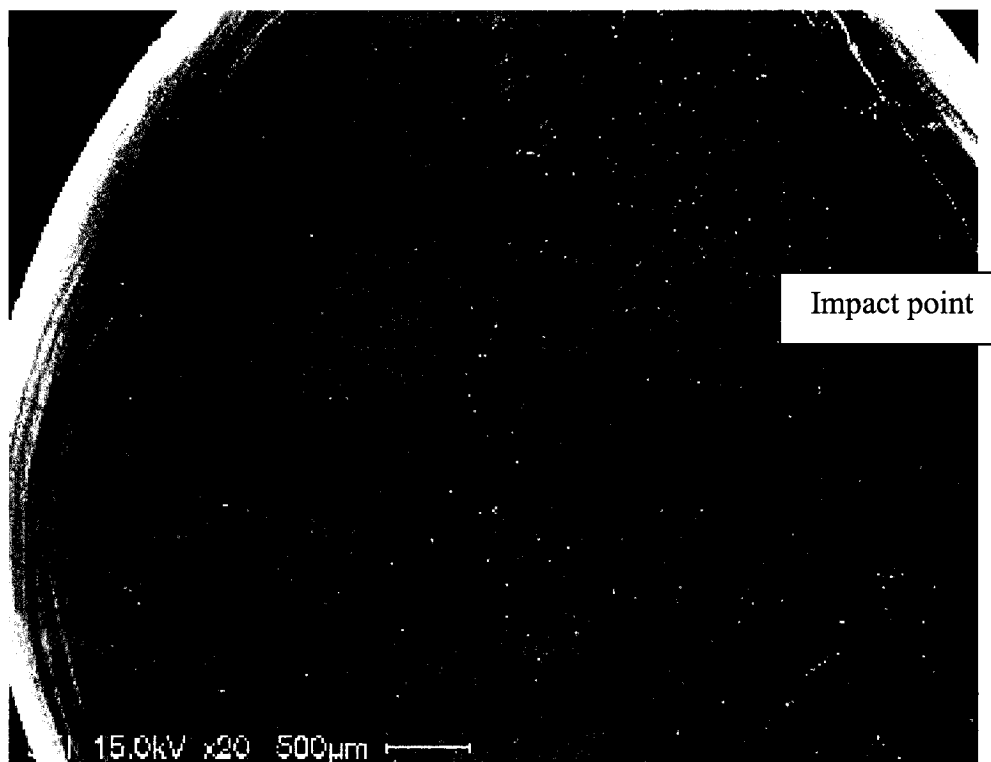


Figure 5.12 – SEM picture of the surface of a droplet that solidified on the polished substrate

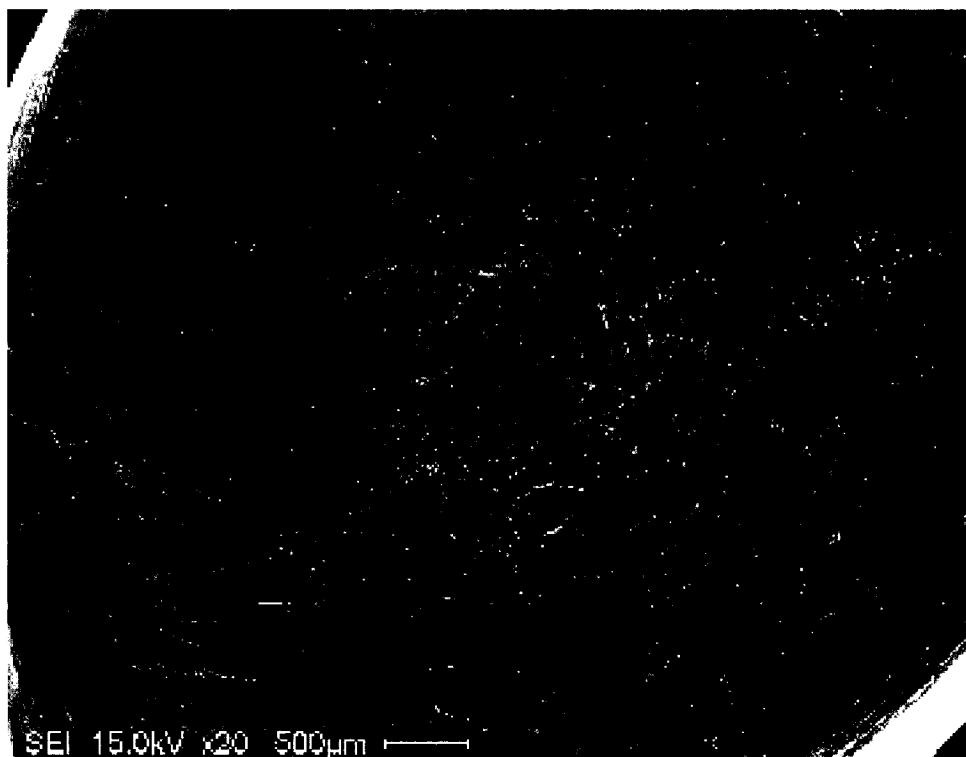


Figure 5.13 - SEM picture of the surface of a droplet that solidified on the sand-blasted substrate

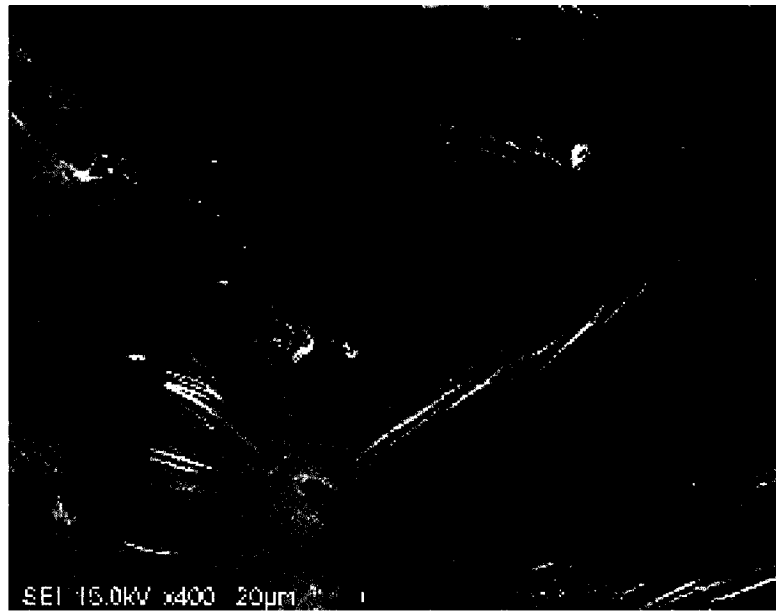


Figure 5.14 – Contact point between the solidifying droplet and the sand-blasted substrate

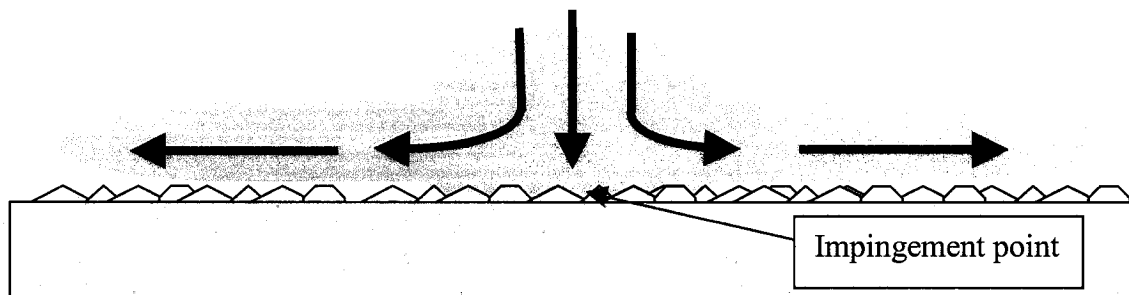


Figure 5.15 – Representation of the droplet spreading after impingement on the sand-blasted surface. The contact at the impingement point is better due to the forces acting vertically.

5.5 – Role of different atmospheres on heat transfer and dynamic wetting

Table 5.4 – Experimental conditions for determining the role of atmospheres on heat transfer and dynamic wetting

	<i>Air</i>	<i>Argon</i>	<i>Helium</i>
<i>Alloy studied</i>	AA1070	AA1070	AA1070
<i>Atmosphere</i>	Air	Argon (0.2% O₂)	Helium (0.2% O₂)
<i>Substrate surface condition</i>	Polished	Polished	Polished
<i>Initial temperature of the substrate</i>	room temp.	room temp.	room temp.
<i>Weight of the droplets</i>	0.34 g	0.34 g	0.34 g
<i>Weber number (We)</i>	3.3	3.3	3.3

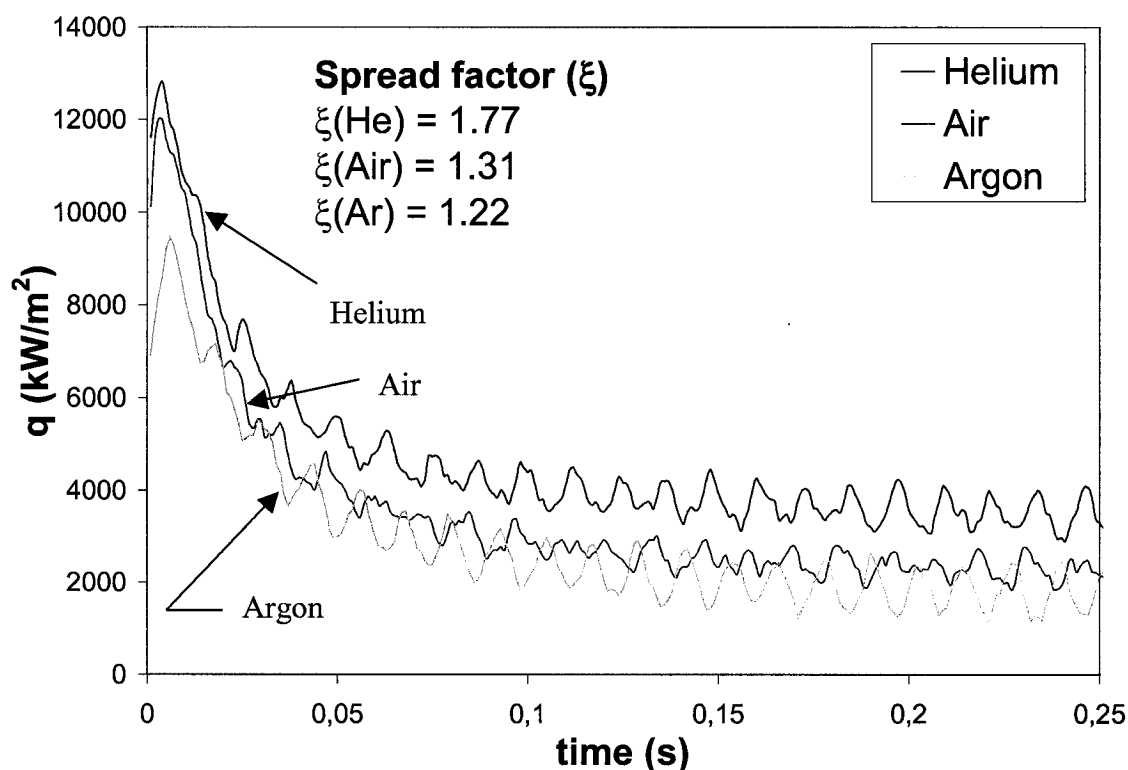
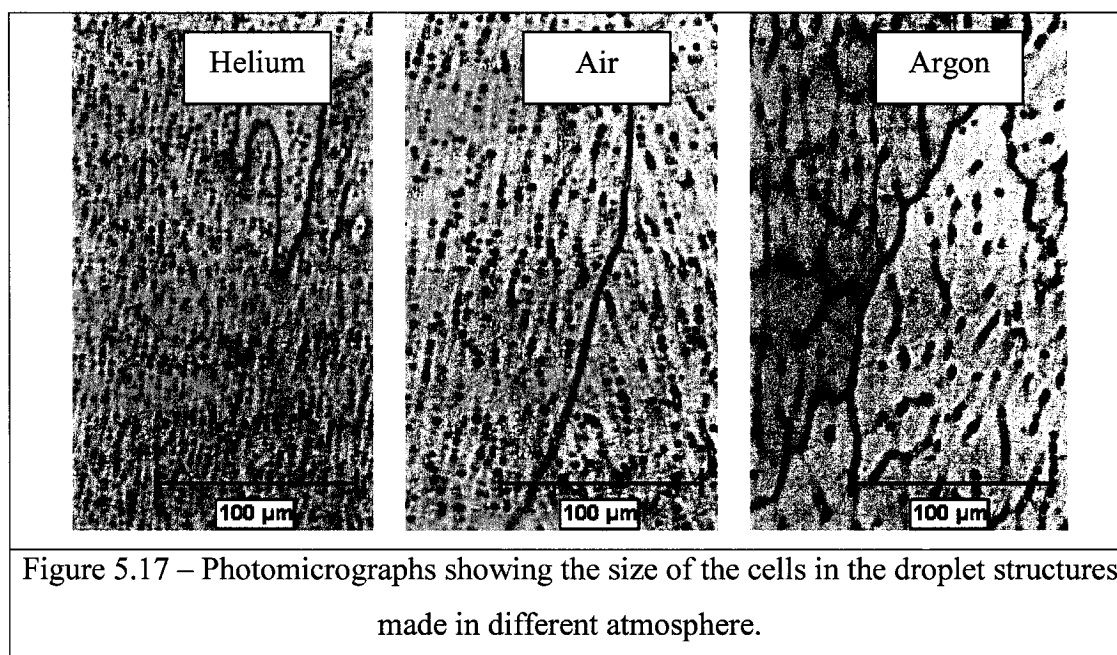


Figure 5.16 – Role of the atmosphere on heat transfer and dynamic wetting

The last parameter studied was the atmosphere used during the formation of the droplets. Pure aluminium droplets were produced in three different atmospheres: argon (with 0.2% O₂), air and helium (with 0.2% O₂). The results were clear and showed a strong dependence of the heat fluxes on the dynamic wetting. The higher was the dynamic

wetting, the higher was the heat transfer. Metallographic analysis was performed on the three sets of droplet to confirm the calculated heat fluxes. These pictures are shown in Figure 5.17. It was concluded from the results that heat transfer and dynamic wetting were higher for droplets made in helium, than in air. Droplets made in argon showed the lowest combination of dynamic wetting and heat transfer.



The results showed previously were for droplets formed in atmospheres of helium and argon with 0.2% O₂. Further experiments were performed to analyse the role of oxygen on wetting and heat transfer. For the second set of droplets, an atmosphere of argon with less than 0.02% O₂ was used. Due to the permeability of the chamber and the smaller molecules of the gas, it was impossible to reach this level of oxygen in a helium atmosphere. The results in the argon atmosphere were very surprising. As seen in Figure 5.18, the aluminium droplet impinged on the substrate (1 ms), spread (7 ms), and then bounced back from the substrate (13 ms). The droplet stayed in the atmosphere for 40 milliseconds, impinged again and then bounced back a second time. In the argon (<0.02% O₂) environment, aluminium droplets showed completely non-wetting conditions.

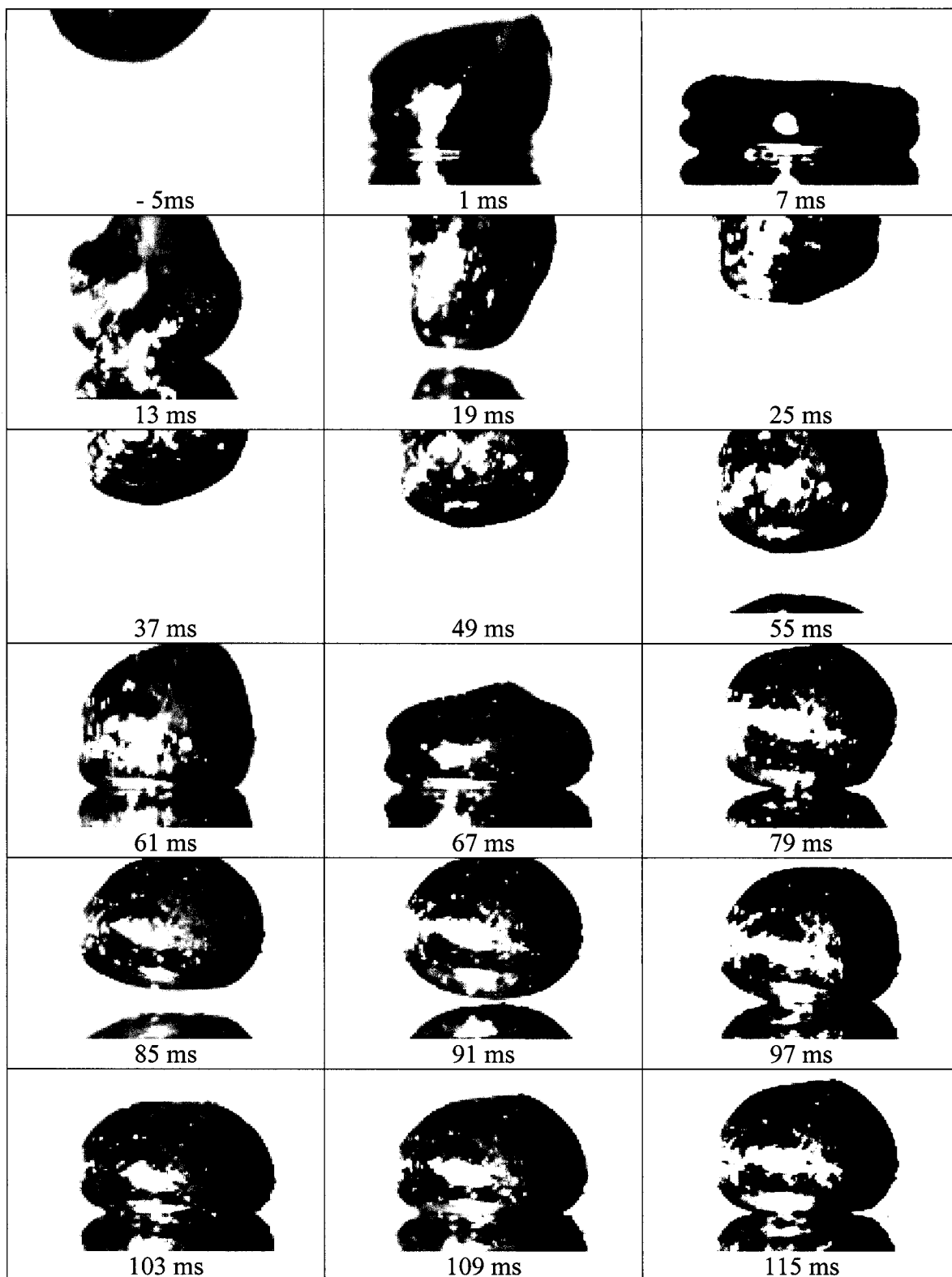


Figure 5.18 – Aluminium droplet impinging, spreading and bouncing back from the substrate in an argon atmosphere of less than 0.02% O₂. (scale 6.5 : 1)

6. CONCLUSIONS AND RECOMMENDATIONS

6.1 – Conclusions

In rapid solidification processes, heat transfer and dynamic wetting are two aspects that can have an impact on the productivity and the quality of the final product. During this project, an experimental set-up was built to study, simultaneously, any links between dynamic wetting and heat transfer for aluminium alloys. Droplets of molten metal were made to impact on a substrate after falling from a prescribed height, while a high-speed camera filmed the sequence of events and thermocouples embedded in the substrate provided data to characterize the heat transfer. Experiments were performed under different conditions and the role of four parameters on dynamic wetting and heat transfer was studied. The results that were obtained have shown that:

- Simultaneous study of the dynamic wetting and heat transfer can be obtained using the drop splat experiment.
- A spreading factor may be used to characterize dynamic wetting.
- Magnesium, as an alloying element in aluminium, was found to increase the dynamic wetting and the initial heat transfer of aluminium droplets.
- Dynamic wetting and heat fluxes were increasing with increasing initial temperature of the substrate.
- For aluminium, roughness of the substrate was found to have an impact on heat transfer. Higher heat fluxes were found using the polished substrate compared to the sand-blasted substrate. Spread factors were numerically equal for both substrate, but a deeper analysis tend to show that a better contact was existing at the droplet/polished substrate interface compared to the rough substrate.

- The gaseous atmosphere was found to affect both heat transfer and dynamic wetting. Higher spread factor and heat fluxes were found in helium, then air, and then argon.
- Aluminium droplets done in an argon atmosphere with less than 0.02% O₂ showed totally non-wetting conditions, since the droplets were bouncing back after hitting the substrate.
- Dynamic wetting and heat transfer appear to be interdependent but as shown in the results presented in this work, the relationship is not always direct. In the majority of the tests that were performed, improved dynamic wetting was associated with increased initial heat fluxes. In some instances the interdependence may have been masked by external factors (e.g. asperities on the substrate).

As mentioned earlier, the set-up that was built in the scope of this project allows the study of dynamic wetting and heat transfer in various industrial processes. The results given in here showed only a general idea of the numerous existing possibilities. The potential combinations of parameters are almost infinite and many other studies could be performed on the subject.

6.2 - Recommendations

As in every research project, some improvements could be performed on the results or the set-up for upcoming works. The following list includes some of the recommendation of progress that should be accomplished in the future.

- Find another material than graphite for the crucible and spindle. As mentioned earlier, the graphite components had to be changed periodically because particles would detach and fall on the substrate.

- Modify the set-up so as to perform experiments for Weber numbers lower, equal and greater than 1. At the moment, the minimum height of fall of the droplets was 4 millimetres. At this height, it was very difficult to acquire images with the camera and it was not possible to determine the impact point of the droplet, making the uncertainty in the heat flux results higher.
- Improve the chamber permeability so that experiments at lower oxygen content could be performed.
- Develop a 2D or 3D heat flow model for the heat fluxes in the substrate. A 1D heat transfer was assumed for the results presented here and was probably not far from reality for the first five millimetres of substrate depth. A 2D or 3D analysis would possibly emphasize the difference in heat fluxes for different conditions found in section 5.2 to 5.5.
- Compare aluminium with other metals having different surface tensions, such as tin, zinc, steel or copper. These metals would give precious information on the influence of the surface tension on dynamic wetting and heat transfer.
- Study the influence of superheat on heat transfer and dynamic wetting.
- Increase roughness of substrates beyond $6.4 \mu\text{m Ra}$.

7. REFERENCES

- [1] Collins, L.E., *Rapid Solidification: How and Why?*, Energy, Mines and Resources Canada, CANMET ed., report (metal technology laboratories (Canada), MTL 88-19 (1988) 23 p.
- [2] Fleetwood, M.J., *Rapid solidification processes*, Met. Mater., 3 (1987) 14.
- [3] Jacobson, L.A., McKittrick, J., *Rapid solidification processing*, Materials Science and Engineering, R11 (1994) 355.
- [4] Ohnaka, I. *State of the Art of Research and Development in Rapid Solidification Technologies in Japan*, Trans. Iron Steel Inst. Jpn., 27 (1987) 919.
- [5] Monteiro, W.A., *Rapid solidification processes in aluminum alloys*, Metalurgia international, 2 (1989) 150.
- [6] Eustathopoulos, N., Nicholas, M.G., Drevet, B., *Wettability at High Temperatures*, Pergamon, New York, NY, USA, (1999).
- [7] Eustathopoulos, N., Coudrier, L., *Influence of alloying elements on wettability and adhesion energy in liquid metal-ceramic systems*, in Contact Angle, Wettability and Adhesion, K.L. Mittal (Ed), (1993) 909.
- [8] Eustathopoulos, N., *Dynamics of wetting in reactive metal/ceramic systems*, Acta mater., 46 (1998) 2319.
- [9] Blake, T.D., *Dynamic contact angles and wetting kinetics*, in Wettability, M. Dekker (Ed), (1993) 251.
- [10] Good, R.J., *Contact angle, wetting, and adhesion: a critical review*, in Contact Angle, Wettability and Adhesion, K.L. Mittal (Ed), (1993) 3.
- [11] Xue, X.M., Wang, J.T., Quan, M.X., *Wettability and spreading kinetics of liquid aluminium on boron nitride*, Journal of Materials Science, 26 (1991) 6391.
- [12] Ho, H.N., Wu, S.T., *The wettability of molten aluminum on sintered aluminum nitride substrate*, Materials Science & Engineering A, A248 (1998) 120.
- [13] Wu, S.T., Wang, D.J., *The influence of oxidation on the wettability of aluminium on sapphire*, Acta mater., 42 (1994) 4029.
- [14] Landry, K., Kalogeropoulou, S., Eustathopoulos, N., *Wettability of carbon by aluminum and aluminum alloys*, Materials Science & Engineering A, A254 (1998) 99.

- [15] Gallois, B.M.; *Wetting in Nonreactive Liquid Metal-Oxide Systems*, JOM, (June 1997) 48.
- [16] Ueda, S., Shi, H., Cramb, A.W., *Observation of the effect of droplet size on the contact angle between liquid iron and a single crystal, alumina substrate at 1873 K*, Iron and Steel Society/AIME, ISSTech 2003 conference proceeding, (2003), 665.
- [17] Ebrill, N., Ph.D. Thesis, University of Newcastle, Callaghan, Australia, (2000).
- [18] Adler, R.P.I., Hsu, S.C., *Dynamic wetting/solidification phenomena*, Rapid Solidification Processing: Principles and Technologies, R. Mehrabian ed., 3 (1983) 448.
- [19] Maringer, R.E., "*Solidification on a Substrate*," Materials Science and Engineering, Vol. 98, 1988, 13-20.
- [20] Dong, S., Niiyama, E., Anzai, K., *Direct observation of deformation of shell solidified at melt-chill contact*, Materials Transactions, JIM, 35 (1994) 196.
- [21] Ulrich, J., Berg, M., Bauckhage, K., *Determination of a splashing threshold for impacting metal droplets using high speed video imaging*, The Minerals, Metals & Materials Society, EPD Congress 1999, B. Mishra ed., (1999) 105.
- [22] Amada, S., Haruyama, M., Ohyagi, T., Tomoyasu, K., *Wettability effect on the flattening ratio of molten metal droplets*, Surface and Coatings Technology, 138 (2001) 211.
- [23] Nishioka, E., Matsubara, T., Fukumoto, M., *Effect of wetting at splat/substrate interface on the flattening behavior of a freely fallen droplet*, Int. J. Materials and Product Technology, Special Issue, SPM1, (2001) 700.
- [24] Ebrill, N., Durandet, Y., Strezov, L., *Dynamic wetting and its influence on interfacial resistance during hot dip galvanizing*, Transactions of the JWRI (Japan), 30 (2001) 351.
- [25] Ebrill, N., Durandet, Y., Strezov, L., *Influence of substrate oxidation on dynamic wetting, interfacial resistance and surface appearance of hot dip coatings*, Verlag Stahleisen GMBH, Galvatech 2001, (2001) 329.
- [26] Ebrill, N., Durandet, Y., Strezov, L., *Dynamic reactive wetting and its role in hot dip coating of steel sheet with an Al-Zn-Si alloy*, Metallurgical and Materials Transactions B, 31B (2000) 1069.
- [27] Beck, J.V., *Nonlinear estimation applied to the nonlinear inverse heat conduction problem*, International Journal of Heat and Mass Transfer, 13 (1970) 703.

- [28] Kim, J.S., Isac, M., Guthrie, R.I.L., Byun, J., *Measurements of interfacial heat transfer resistances and characterization of strip microstructures for Al-Mg alloys cast on a single belt casting simulator*, Light Metals 2000 Métaux Légers, Canadian Institute of Mining, Metallurgy and Petroleum (2000) 635.
- [29] Tavares, R.P., Isac, M., Hamel, F.G., Guthrie, R.I.L., *Instantaneous interfacial heat fluxes during the 4 to 8 m/min casting of carbon steels in a twin-roll caster*, Metallurgical and Materials Transactions B, 32B (2001) 55.
- [30] Guthrie, R.I.L., Isac, M., Kim, J.S., Tavares, R.P., *Measurements, simulations, and analyses of instantaneous heat fluxes from solidifying steels to the surfaces of twin roll casters and of aluminium to plasma-coated metal substrates*, Metallurgical and Materials Transactions B, 31B (2000) 1031.
- [31] Strezov, L., Herbertson, J., Belton, G.R., *Mechanisms of initial melt/substrate heat transfer pertinent to strip casting*, Metallurgical and Materials Transactions B, 31B (2000) 1023.
- [32] Strezov, L., Herbertson, J., *Experimental studies of interfacial heat transfer and initial solidification pertinent to strip casting*, ISIJ International, 38 (1998) 959.
- [33] Bouchard, D., Hamel, F.G., Nadeau, J.P., Bellemare, S., Dreneau, F., Tremblay, D.A., Simard, D., *Effects of substrate surface conditions on heat transfer and shell morphology in the solidification of a copper alloy*, Metallurgical and Materials Transactions B, 32B (2001) 111.
- [34] Bouchard, D., Howes, B., Paumelle, C., Nadeau, J.P., Simard, D., *Control of heat transfer and growth uniformity of solidifying copper shells through substrate temperature*, Metallurgical and Materials Transactions B, 33B (2002) 403.
- [35] Misra, P., Phininchka, N., Cramb, A.W., *The effect of the presence of liquid films on a copper mold surface on the rate of heat transfer during the solidification of steel droplets*, Iron and Steel Society/AIME, ISSTech 2003 conference proceeding, (2003), 263.
- [36] Liu, W., Wang, G.X., Matthys, E.F., *Determination of the thermal contact coefficient for a molten droplet impinging on a substrate*, HTD, 196 (1992) 111.
- [37] Liu, W., Wang, G.X., Matthys, E.F., *Thermal analysis and measurements for a molten metal drop impacting on a substrate: cooling, solidification and heat transfer coefficient*, International Journal of Heat and Mass Transfer, 38 (1995) 1387.
- [38] Wang, G.X., Matthys, E.F., *Experimental determination of the interfacial heat transfer during cooling and solidification of molten metal droplets impacting on a metallic substrate: effect of roughness and superheat*, International Journal of Heat and Mass Transfer, 42 (1999) 2129.

- [39] Todoroki, H., Lertarmon, R., Cramb, A.W., Suzuki, T., *Initial solidification of iron, nickel and steel droplets*, Iron and Steelmaker, 26 (1999) 57.
- [40] Todoroki, H., Lertarmon, R., Suzuki, T., Cramb, A.W., *Heat transfer behavior of pure iron and nickel against a water cooled copper mold during initial stage of solidification*, Iron and Steel Society/AIME, Steelmaking Conference Proceedings, 80 (1997) 667.
- [41] Todoroki, H., Lertarmon, R., Suzuki, T., Cramb, A.W., *Solidification and heat transfer behavior of 304 stainless steel*, Minerals, Metals and Materials Society/AIME, (1997) 2227.
- [42] Loulou, T., Artyukhin, E.A., Bardon, J.P., *Estimation of thermal contract resistance during the first stages of metal solidification process: II – experimental setup and results*, International Journal of Heat and Mass Transfer, 42 (1999) 2129.
- [43] Loulou, T., Bardon, J.P., *Heat transfer during the spreading and solidification of a molten metal droplet on a cooled substrate*, High Temperature Material Processes, 4 (2000) 69.
- [44] Evans, T., Strezov, L., *Interfacial heat transfer and nucleation of steel on metallic substrates*, Metallurgical and Materials Transactions B, 31B (2000) 1081.
- [45] American Society of Metallurgy (ASM), Metals Handbook, Desk Edition, 1991.
- [46] Zhang, L., Taniguchi, S., *Fundamentals of inclusion removal from liquid steel by attachment to rising bubbles*, The Iron and Steel Society, (2001) 55.
- [47] Mizukami, H., Suzuki, T., Umeda, T., *Tetsu-to-Hagané*, 78 (1992) 1369.
- [48] Muojekwu, C.A., Samarasekera, I.V., Brimacombe, J.K., *Heat transfer and microstructure during the early stages of metal solidification*, Metallurgical and Materials Transactions B, 26B (1995) 361.
- [49] Lang, G., *Effect of added elements on the surface tension of high purity aluminium*, Aluminium, vol. 50-1 (1974) 731-734.
- [50] Barralis, J.; Maeder, G.; *Précis de métallurgie*, Nathan, Paris, 2000.
- [51] Brandes, E.A., Brook, G.B., *Smithells Metals Reference Book*, 7th ed., Butterworth-Heinemann, Oxford, United Kingdom, 1992, p. 14-1.
- [52] Gaskell, D.R., *Introduction to the Thermodynamics of Materials*, 3rd ed., Taylor & Francis, USA, (1995).

- [53] Guthrie, R.I.L., *Engineering in Process Metallurgy*, Oxford Science Publications, (2002).
- [54] Holman, J.P., *Heat transfer*, 8th ed, McGraw Hill inc., New York, (1997).
- [55] Iida, T., Guthrie, R.I.L., *The Physical Properties of Liquid Metals*, Oxford University Press, Toronto, ON, Canada, (1988).
- [56] Kubaschewski, O., Alcock, C.B., Spencer, P.J., *Materials Thermochemistry*, 6th ed., 1993, Pergamon Press Ltd., New York, NY, p. 274.
- [57] Li, G., Thomas, B.G., *Transient thermal model of the continuous single-wheel thin-strip casting process*, Metallurgical and Materials Transactions B, 27B (1996) 509.
- [58] Massey, B.S., *Mechanics of Fluids*, Van Nostrand Reinhold editor, (1980).
- [59] Özisik, M.N., *Heat Conduction*, John Wiley and sons, New York, (1980).
- [60] Touloukian, Y.S., Powell, R.W., Ho, C.Y., Klemens, P.G., *Thermophysical Properties of Matter*, Plenum Publishing Corp., New York, NY, 1970, vol. 1, p. 81.
- [61] Bouchard, D., Hamel, F.G., Turcotte, S.F., Nadeau, J.P., *Water Modeling Evaluation of Metal Delivery in a Twin Roll Strip Caster Using Pool Level and Residence Time Distribution Measurements*, ISIJ International, 41 (2001) 1465.

APPENDIX – Conference of metallurgists of CIM, Vancouver, 2003**Aluminium droplets impinging on a copper substrate: a dynamic wetting and heat transfer study.**

Sébastien Leboeuf, Dominique Bouchard and Jean-Paul Nadeau
Aluminium Technology Centre
75 de Mortagne Boulevard
Boucherville, Québec, Canada, J4B 6Y4

Roderick I. L. Guthrie and Mihaiela Isac
McGill Metals Processing Centre, McGill University
3610 University Street, M.H. Wong Building
Montréal, Québec, Canada, H3A 2B2

ABSTRACT

The present work describes an experimental set-up built to simulate dynamic wetting and heat transfer occurring in many rapid solidification processes. Tests were performed with molten aluminium droplets falling from a crucible onto a metallic substrate. A high-speed camera captured the evolution of the droplet's geometry, while thermocouples, inserted inside the metallic substrate, allowed a heat transfer analysis to be performed. The results that were obtained are presented and discussed.

A copy of this paper was published in the *Proceedings of the International Symposium on Light Metals 2003 Métaux Légers* (J. Masounave and G. Dufour editors) and presented at the 42nd Conference of Metallurgists of CIM in Vancouver

INTRODUCTION

Wetting and heat transfer are two important aspects of rapid solidification processes. In twin-roll strip casting, they have a major impact on the quality of the final product and on the productivity of the process. Recently, the Aluminium Technology Centre (ATC) has undertaken a research program to evaluate the castability of aluminium and its alloys with a vertical twin roll caster. In this process, liquid aluminium wets the surface of two rotating rolls that are water-cooled and heat is transferred so as to solidify strips. Improper wetting and/or heat transfer can result in non-uniform solidification and surface cracks.

Small-scale laboratory set-ups can be used to characterize wetting and heat transfer. For example, wetting between a liquid and a solid is often studied with the sessile drop technique. The wettability is provided by the contact angle between a liquid droplet and a solid substrate (1). However, these experiments require thermodynamic equilibrium and a time scale of 100 seconds or more is normally necessary to make the measurements. These conditions do not reflect those found in twin roll casting where there is an absence of equilibrium. Moreover, liquid metal is in contact with the rolls for a period in the order of 1 millisecond before it solidifies and wetting thus occurs under dynamic, rather than static conditions.

Adler et al. (2) and Maringer (3) have been among the first to acknowledge the importance of dynamic wetting in solidification processes. By carrying out experiments with liquid metallic droplets that solidified after they impinged on substrates, they showed that adherence between the droplet and the substrate was instrumental in the heat transfer. These drop-splat experiments also showed the influence of surface conditions, and initial temperatures of the substrate, on adherence.

Dong et al. (4) used a similar approach to study the deformation of melts (pure Pb, Bi, Sn and alloys) on a chill substrate during solidification. They studied this phenomenon using a camera operating at 500 to 1000 frames/second. The authors concluded that the instantaneous deformations of solidifying metals could explain the presence of certain defects on the cast surfaces of some rapid solidification processes.

Ebrill et al. (5,6), studied both dynamic wetting and interfacial heat fluxes using two different set-ups. For dynamic wetting, they used an experimental apparatus similar to those cited above and the evolution of the wetting angle of the solidifying droplets was captured using a high-speed camera. The authors demonstrated the influence of initial temperature of the substrate on dynamic wetting; the latter being improved as the substrate temperature approached the melting point of the molten metal. Interfacial heat fluxes were measured by dipping substrates into a bath of molten alloy.

The drop-splat set-ups for dynamic wetting experiments have also been used to characterize heat transfer. Todoroki (7) inserted thermocouples inside the substrates to measure the temperature evolution as the droplets solidified and evaluated the interfacial heat transfer coefficients along with heat fluxes. Surface conditions of the substrates, superheat of the molten metals and alloy compositions, were found to influence the heat transfer. A similar analysis has also been carried out using temperature measured with pyrometers (8,9).

Although it has been shown that the drop-splat set-up is suited to study dynamic wetting and heat transfer at the initiation of solidification, the set-up has never been used to analyse the two phenomena during the same experiment. It is often assumed that improved dynamic wetting promotes heat transfer but this is best demonstrated by simultaneously characterizing both phenomena. This paper describes work carried out at the Aluminium Technology Centre and provides the preliminary results on the dynamic wetting and heat transfer of solidifying aluminium droplets.

EXPERIMENTAL

The experimental set-up constructed in this work is similar to the one of Ebrill et al. (5,6) and Todoroki et al (7). Figure 1 is a depiction of the apparatus. It consisted of a copper substrate, a graphite crucible with a small hole at the bottom, a spindle made of graphite, a resistance heating element, an electric motor, a moving table and a high-speed camera (10 000 frames/second).

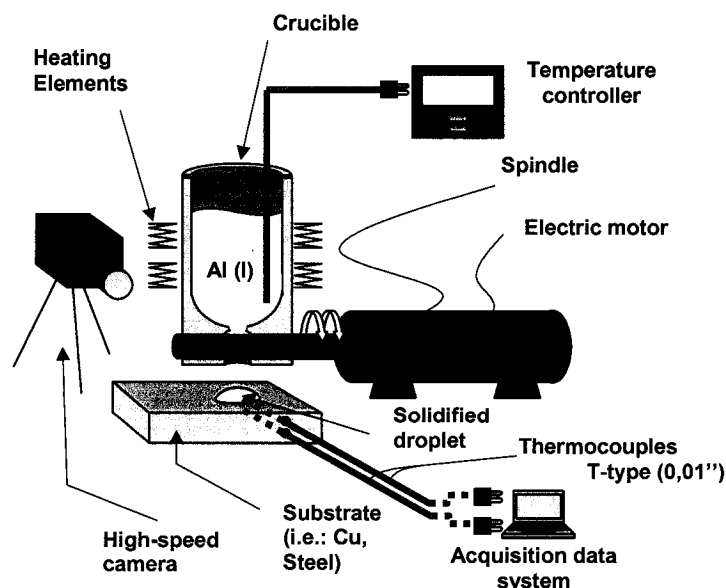


Figure 1 – Experimental Set-Up for the Simultaneous Characterization of Dynamic Wetting and Heat Transfer at the Initiation of Solidification of Aluminium.

The copper substrate (50 mm x 50 mm x 20 mm) had a purity of 99.9+ percent and an average surface roughness (Ra) of 0.2 μm . Typically, 200 grams of pure aluminium (AA 1070) were melted and kept at 725 $^{\circ}\text{C}$ in the graphite crucible (155 mm high, 75 mm in diameter). Graphite was chosen for its non-wetting and non-reacting properties toward aluminium, as well as for its good machinability. An electric motor was used to rotate the spindle in which a dimpled cavity was machined. As it faced the small hole at the bottom end of the crucible, this cavity was filled with liquid aluminium and a molten droplet formed following rotation of the spindle. Then, the droplet was released under free-fall conditions, impinged on the copper-substrate, and solidified. Droplet volumes were determined by the dimple's size. Two T-type thermocouples (0.25 mm) were inserted in the centre of the substrate, one 1 mm below the surface, and the other at 5 mm. These thermocouples measured the evolution of temperature at a frequency of 1000 Hz. The moving table on which the electric motor and crucible were lying could be displaced in the x, y and z directions, this allowed experiments to be carried out for different heights and positions. The whole set-up was enclosed in a chamber gas to provide a controlled atmosphere. Finally, the high-speed camera captured the evolution in the shape of the droplet as it spread on the substrate. The images taken by the camera were analysed simultaneously with the data acquired for heat transfer.

THEORY

When a droplet falls and impinges on a substrate, the main forces that are present are: inertial, gravitational, viscous and surface tension. Among them, inertial and surface tension forces play an important role in the evolution of the shape of the droplet as it collides with the substrate. The ratio of inertial to surface tension forces is given by the dimensionless Weber number, We , expressed as:

$$We = \frac{\rho U_o^2 L}{\sigma} \quad (1)$$

As soon as the droplet contacts the surface of the substrate, heat transfer is initiated. For the splat, heat transfer by unidirectional conduction predominates over convection and radiation (10). In this work, only the heat flow into the substrate was accounted for and this is described with the transient equation:

$$\rho \cdot C \cdot \frac{\partial T}{\partial t} = \frac{\partial}{\partial x} \left(k_x(T) \frac{\partial T}{\partial x} \right) \quad (2a)$$

having the following initial and boundary conditions:

$$T(x,0) = T_o \quad 0 \leq x \leq N \quad (2b)$$

$$-k \left. \frac{\partial T}{\partial x} \right|_{x=N} = 0 \quad t \geq 0 \quad (2c)$$

$$-k \left. \frac{\partial T}{\partial x} \right|_{x=0} = q(t) \quad t \geq 0. \quad (2d)$$

Heat fluxes entering the substrate were calculated by solving the function-specification method proposed by Beck (11). The detailed description of this method has been presented elsewhere (11,12) and only a brief description is given here.

The contact time between the droplet and the substrate was divided into m individual intervals. The heat flux was considered to be constant within each interval, but to vary from one to another. The heat flux was found by iteration using the following formula:

$$q_m^{n+1} = q_m^n + \frac{\sum_{i=1}^r \sum_{j=1}^J (Y_{m+i-1,j} - T_{m+i-1,j}(q_m^n)) \cdot \frac{T_{m+i-1,j}(q_m^n(1+\delta)) - T_{m+i-1,j} \cdot q_m^n}{\delta q_m^n}}{\sum_{i=1}^r \sum_{j=1}^J \left(\frac{T_{m+i-1,j}(q_m^n(1+\delta)) - T_{m+i-1,j} \cdot q_m^n}{\delta q_m^n} \right)^2} \quad (3a)$$

where $Y_{m+i-1,j}$ is a measured temperature at the time interval $m+i-1$, $T_{m+i-1,j}(q_m^n)$ and $T_{m+i-1,j}(q_m^n(1+\delta))$ are temperatures calculated by solving the direct problem when fluxes q_m^n and $q_m^n(1+\delta)$ are imposed at the surface of the substrate. The fixed value increment δ for q_m^n was chosen to be 0.001. J represents the number of thermocouples, r is the number of future time steps and n is the n^{th} iteration. Iterations were begun with an initial value for q_m^n , and performed until the following condition was met:

$$\frac{q_m^{n+1} - q_m^n}{q_m^n} \leq 0.005. \quad (3b)$$

RESULTS AND DISCUSSION

The metallographic structure of a droplet solidified with the present set-up is shown in Figure 2. The chill and columnar zones, typical of unidirectional heat flow at the start of solidification, are easily identified, as is the presence of an equiaxed zone near the top surface of the solidified droplet.

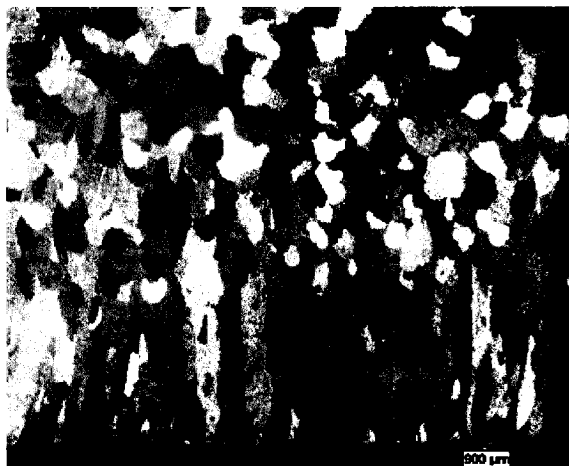


Figure 2 – Ingot structure of a droplet. Heat transfer proceeded unidirectionally from bottom to top. The chill, columnar and equiaxed zones can be well identified (1 g, height of fall = 12mm, atmosphere = air).

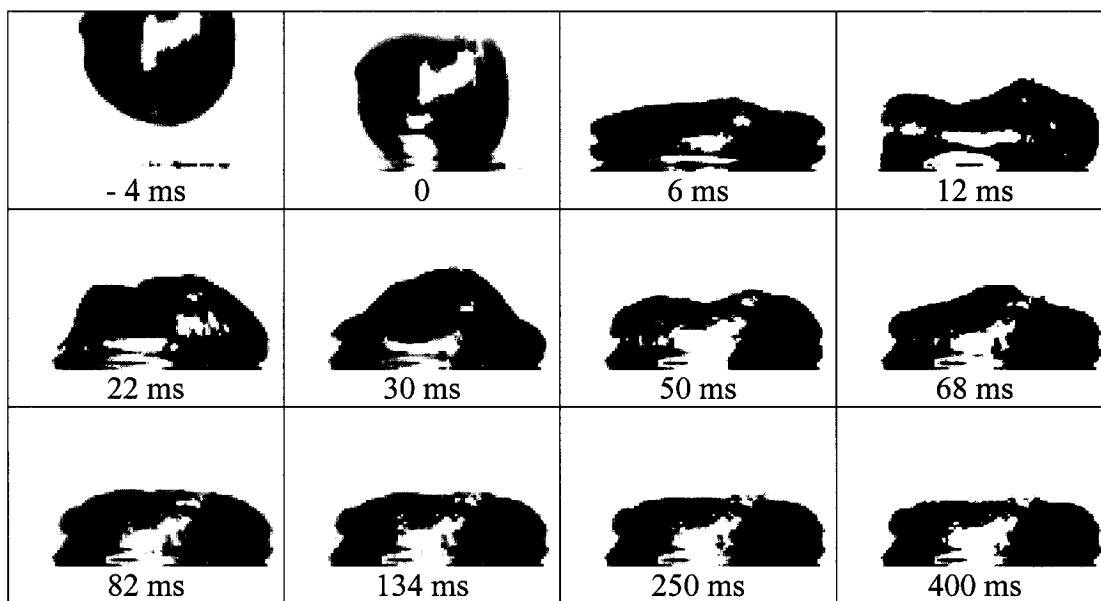


Figure 3 – Droplet Impinging on a Substrate Surface (0.42 g, height of fall = 10mm)

Experiments were carried out in air at four different heights of fall and repeated four times. Figure 3 illustrates the interaction of the droplet with the substrate. The droplet first impacted and then spread out on the substrate. As solidification proceeded, liquid metal in the droplet was constantly moving and the top surface was oscillating. Solidification was completed after approximately 0.4 second.

Temperatures obtained by the thermocouples inserted in the substrate are shown in Figures 4,5,6 and 7. The one at 1 mm was always more sensitive than the other at 5

mm. As shown in Figures 4 to 7, there was a time interval of 30 milliseconds between the rise in temperature read by the thermocouple at 1 mm and the one at 5 mm. For example, in Figure 4, the temperature started rising at 1.095 seconds for the first thermocouple and at 1.125 seconds for the second.

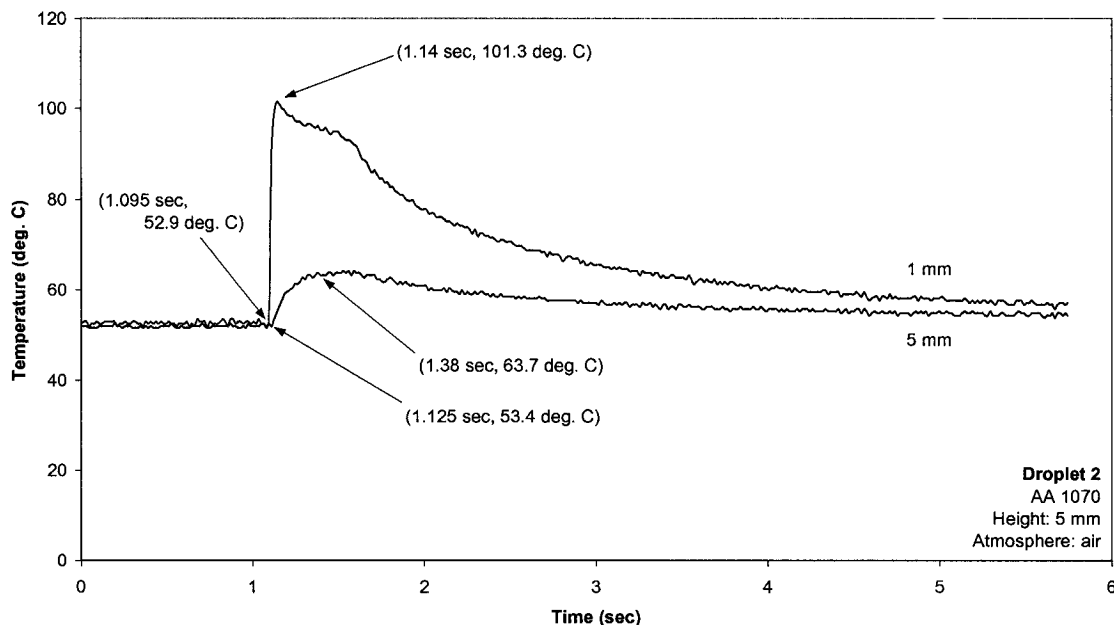


Figure 4 – Temperature Profiles in the Substrate for a Droplet Falling from a Height of 5 mm

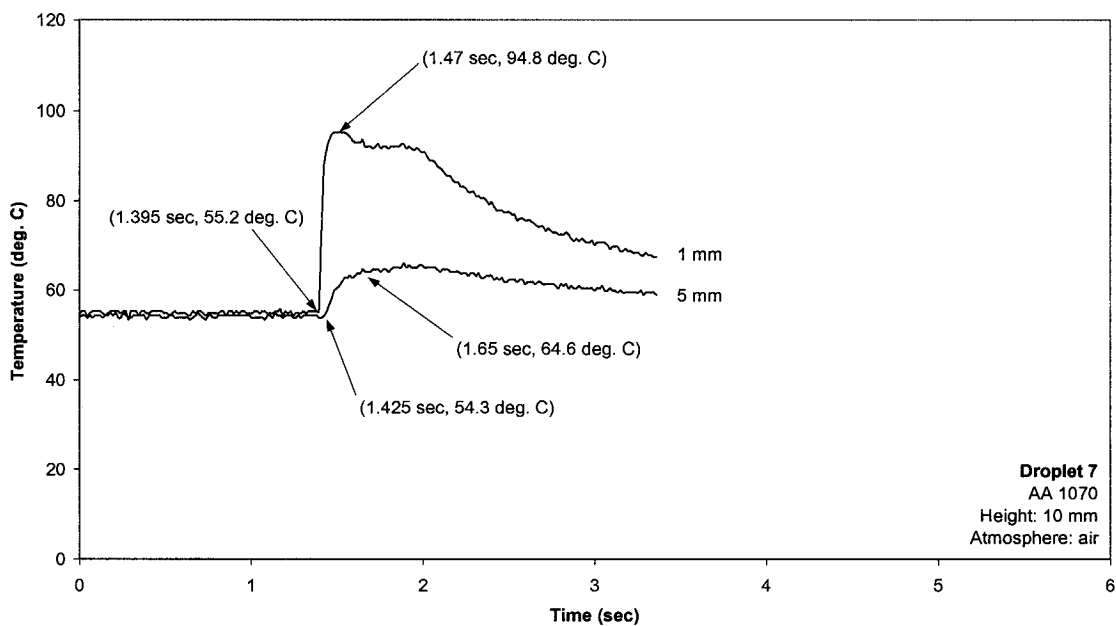


Figure 5 – *Idem* to Figure 4 for a Height of 10 mm

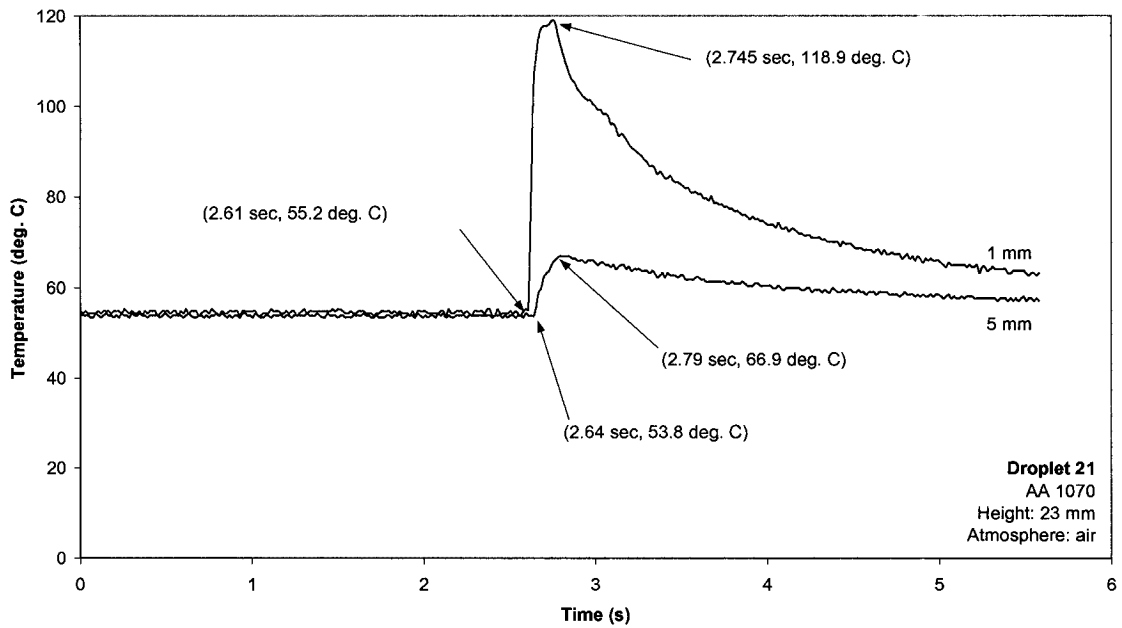


Figure 6 – *Idem* to Figure 4 for a Height of 23 mm

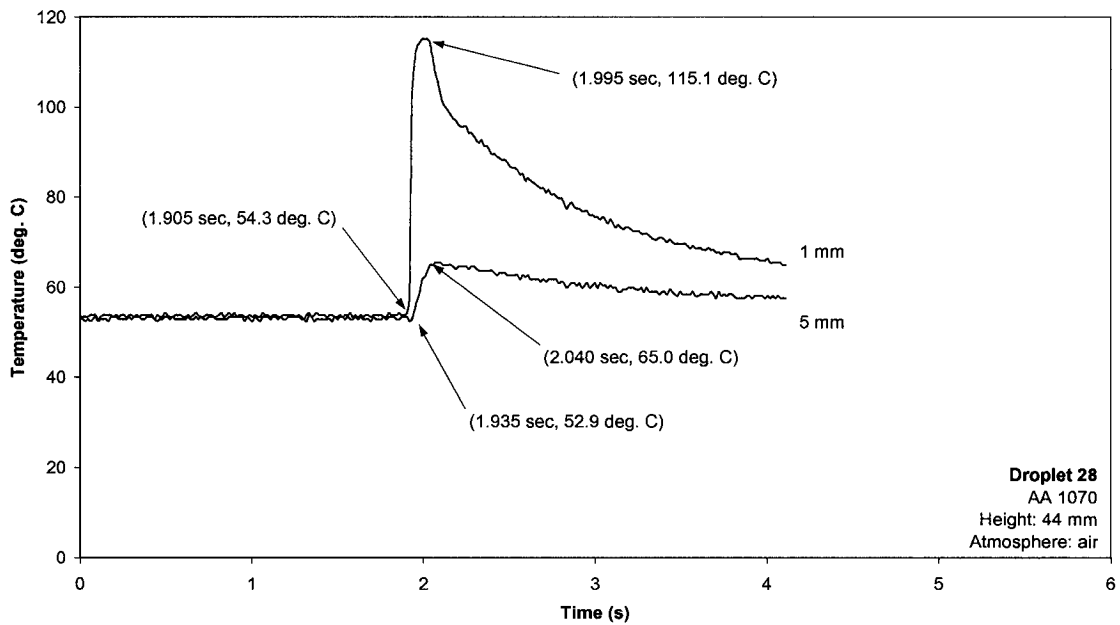


Figure 7 – *Idem* to Figure 4 for a Height of 44 mm

Figures 8 to 11 show the heat flux evolutions and the concurrent shapes of the droplet at specific times. It is considered that the correspondence between the heat fluxes and the shapes of the droplets are within ± 2 milliseconds.

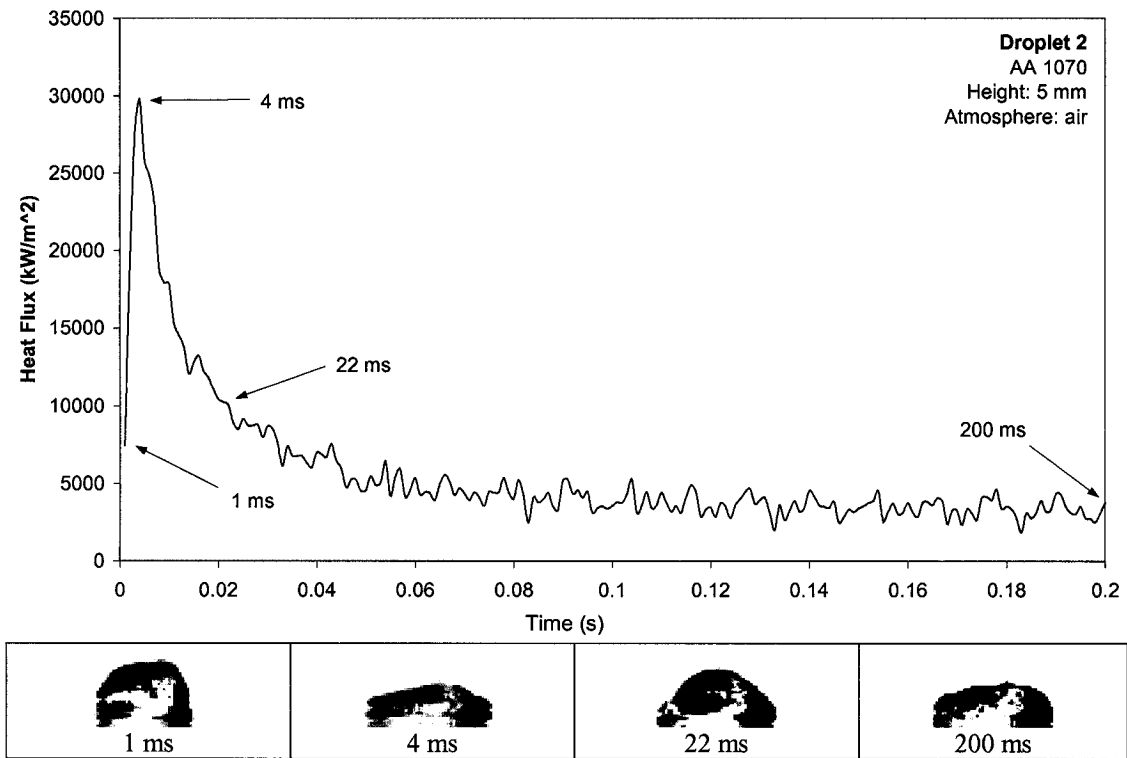


Figure 8 – Heat Flux as a Function of Time and Sequence of the Droplet Impinging, Wetting and Spreading at Specific Times for a Height of Fall of 5 mm.

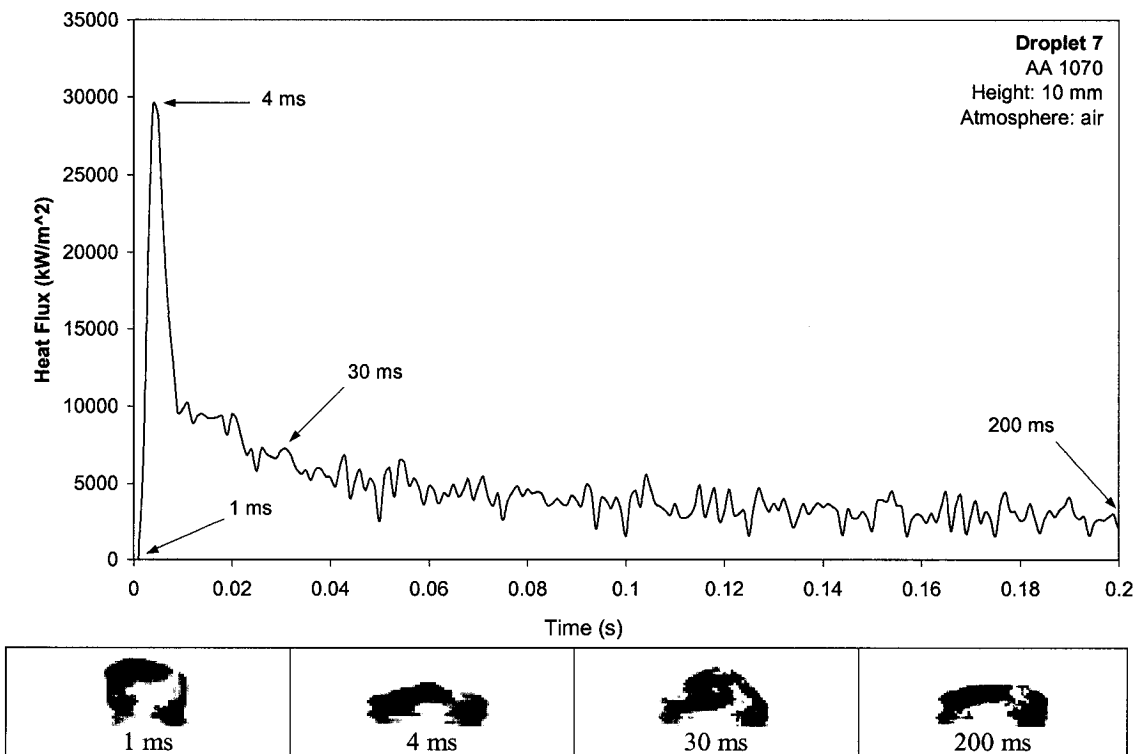


Figure 9 – *Idem* to Figure 8 for a Height of Fall of 10 mm

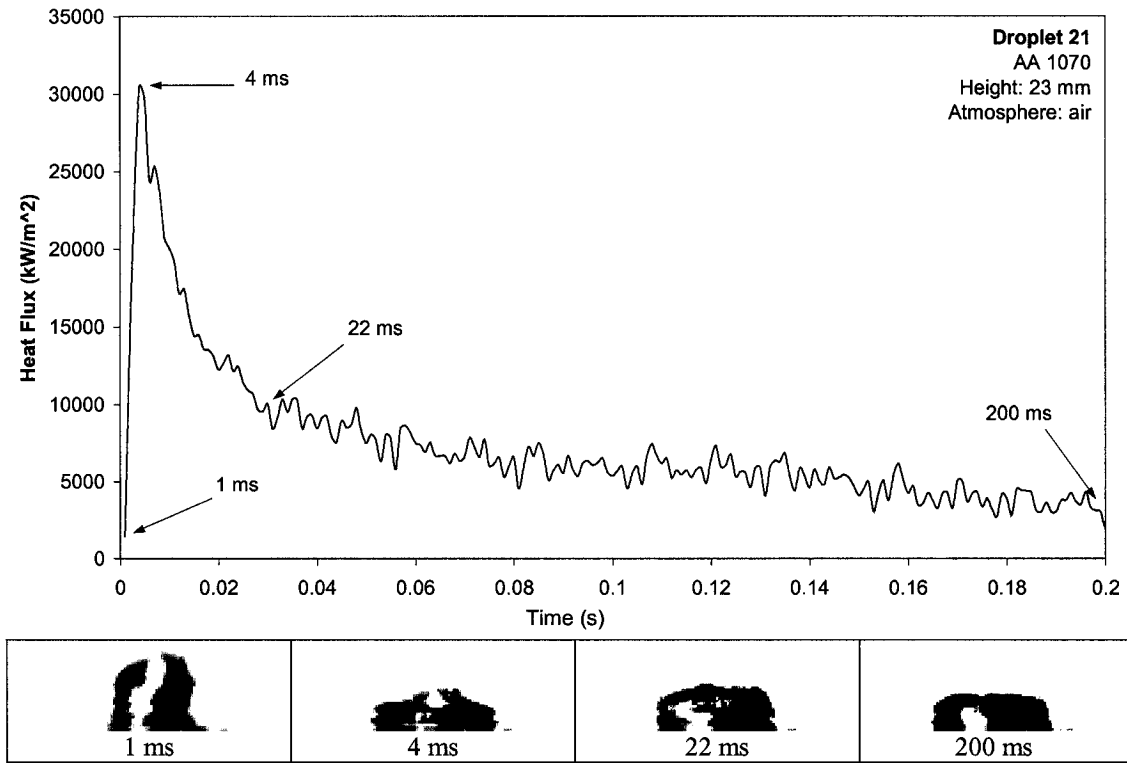


Figure 10 – *Idem* to Figure 8 for a Height of Fall of 23 mm

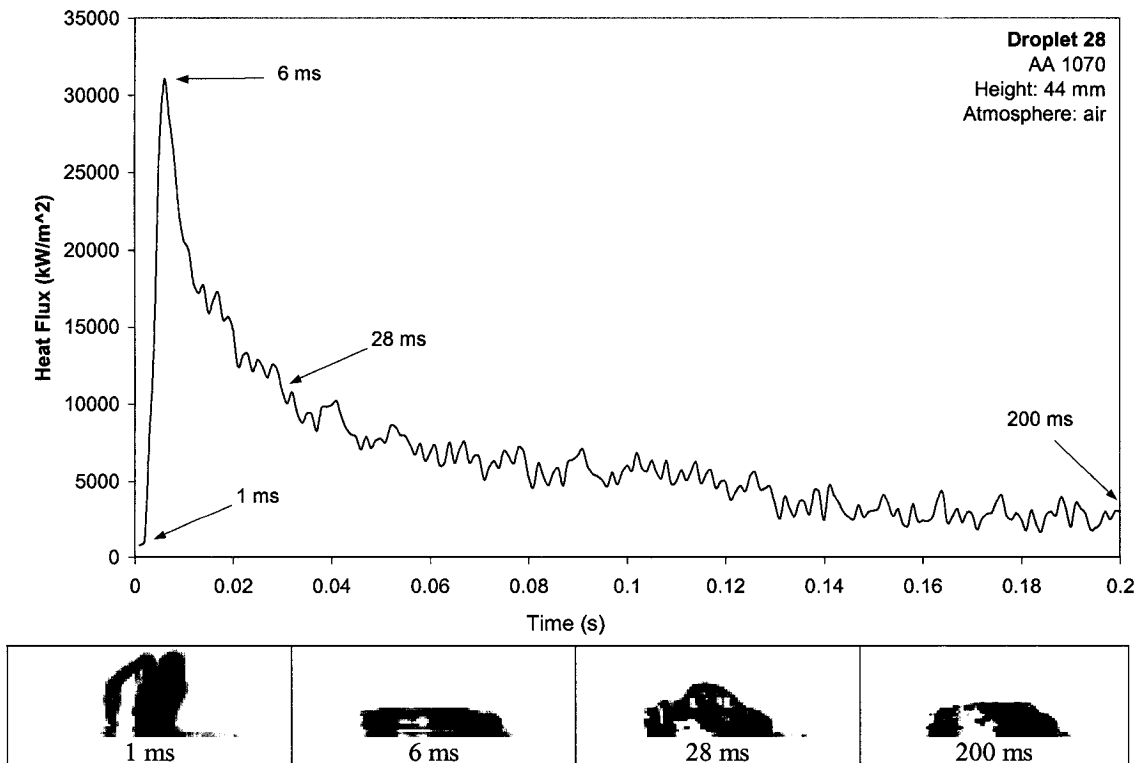


Figure 11 – *Idem* to Figure 8 for a Height of Fall of 44 mm

The results in these figures indicate that the heat flux rose as the contact area between the substrate and the droplet increased and the peak value in the heat flux was established once spreading was completed. Also, an increase in the height of fall was associated with a smaller thickness and larger diameter of the solidified droplet. Figure 12 illustrates the average heat fluxes for each height. The initial time on this graph, ($t = 0$), was obtained from the change in the slope of temperature evolution in the substrate.

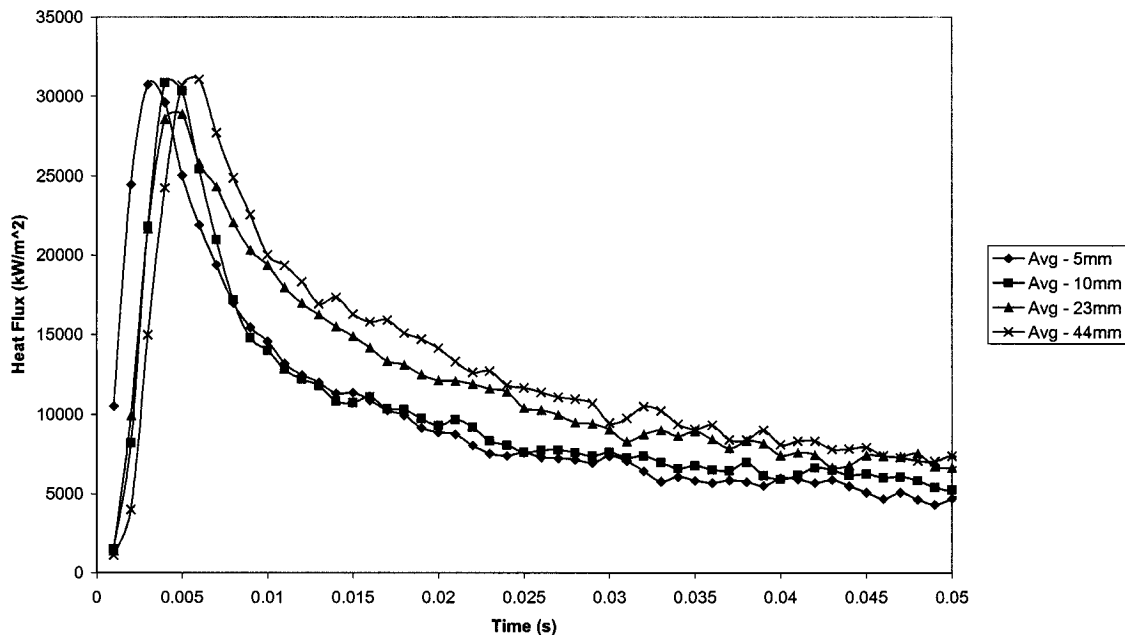


Figure 12 – Comparison Between the Average Heat Flux Curves for Droplets Falling from Four Different Heights.

For the droplets falling from 5, 10, 23 and 44 mm the corresponding Weber numbers were respectively: 1.8, 3.6, 8.2 and 15.7. The physical properties required to calculate these numbers were taken from Iida and Guthrie (13). As the ratio of inertial to surface tension forces increased, the effect on the heat transfer curves was to shift their peak values slightly to the right. The increase in the ratio of these forces also influenced the evolution of the shapes of the droplets (Figures 8 to 11) but the effect on the actual contact angles still needs to be carried out to determine if the results reported here also apply when surface tension predominates ($We < 1$). The experimental set-up and procedure described in this paper will be used to determine the effect of several factors on dynamic wetting and heat transfer, for example, composition of the gaseous atmosphere, substrate conditions, alloy compositions, etc. The evolution in the contact angles of the droplets with the substrates will also be quantified to compare with that for the heat fluxes.

CONCLUSION

An experimental set-up was constructed to simultaneously characterize dynamic wetting and heat transfer in the early stages of aluminium solidification. Droplets of molten metal were made to impact on a substrate after falling from a prescribed height while a high-speed camera filmed the sequence of events and thermocouples embedded in the substrate provided data to characterize the heat transfer. The results that were obtained have shown that spreading follows impact of the droplet with the substrate and that the end of this spreading coincides with a peak in the heat flux. Increasing the height of fall delayed the time at which the peak heat flux occurred.

ACKNOWLEDGEMENTS

Technical assistance from Daniel Simard and Martin Pruneau is acknowledged.

NOMENCLATURE

We	Weber number
ρ	density [$\text{kg}\cdot\text{m}^{-3}$]
U_o	final velocity of the droplet before impacting with substrate [$\text{m}\cdot\text{s}^{-1}$]
L	droplet diameter [m]
σ	surface tension [$\text{kg}\cdot\text{s}^{-2}$]
C	heat capacity [$\text{kJ}\cdot\text{kg}^{-1}\cdot\text{K}^{-1}$]
T	temperature [K]
T_o	initial temperature [K]
t	time [s]
x	length [m]
k	thermal conductivity [$\text{W}\cdot\text{m}^{-1}\cdot\text{K}^{-1}$]
N	total number of nodes
m	number of time intervals
n	iteration number in Eqs. (6) and (7)
i	node identification in the numerical analysis
r	number of future time-steps
J	total number of thermocouples
Y	measured temperatures [K]
δ	incremental heat flux factor

REFERENCES

1. N. Eustathopoulos, M.G. Nicholas and B. Drevet, Wettability at High Temperatures, Pergamon, New York, NY, USA, 1999.
2. R.P.I. Adler and S.C. Hsu, "Dynamic Wetting/Solidification Phenomena," Rapid Solidification Processing: Principles and Technologies Vol. 3, R. Mehrabian, Ed., 1983, 448-451.
3. R.E. Maringer, "Solidification on a Substrate," Materials Science and Engineering, Vol. 98, 1988, 13-20.
4. S. Dong, E. Niiyama and K. Anzai, "Direct Observation of Deformation of Shell Solidified at Melt-Chill Contact," Materials Transactions, Vol. 35, No. 3, 1994, 196-198.
5. N. Ebrill, Y. Durandet and L. Strezov, "Dynamic Reactive Wetting and its Role in Hot Dip Coating of Steel Sheet with an Al-Zn-Si Alloy," Metallurgical and Materials Transactions B, Vol. 31B, 1069-1079.
6. N. Ebrill, Y. Durandet and L. Strezov, "Dynamic Wetting and its Influence on Interfacial Resistance During Hot Dip Galvanizing," Transactions of the JWRI (Japan), Vol. 30, 2001, 351-359.
7. H. Todoroki, R. Lertarom, T. Suzuki and A.W. Cramb, "Heat Transfer behavior of Pure Iron and Nickel Against a Water Cooled Copper Mold During Initial Stage of Solidification," Steelmaking Conference Proceedings, Vol. 80, Iron and Steel Society of AIME, Warrendale, PA, USA, 1997, 667-678.
8. W. Liu, G.X. Wang and E.F. Matthys, "Thermal Analysis and Measurements for a Molten Metal Drop Impacting on a Substrate: Cooling, Solidification and Heat Transfer Coefficient," Int. J. Heat Mass Transfer, Vol. 38, No. 8, 1995, 1387-1395.
9. T. Evans and L. Strezov, "Interfacial Heat Transfer and Nucleation of Steel on Metallic Substrates" Metallurgical and Materials Transactions B, Vol. 31B, October 2000, 1081-1089.
10. B.G. Thomas and J.T. Parkman, "Simulation of Thermal Distortion of a Steel Droplet Solidifying on a Copper Chill," Solidification and Deposition of Molten Metal Droplets, M. Chu and E. Lavernia Eds., TMS, Warrendale, PA, USA, 1998, pp. 509-520.

11. J.V. Beck, "Nonlinear Estimation Applied to the Nonlinear Inverse Heat Conduction Problem," Int. J. Heat Mass Transfer, Vol. 13, 1970, 703-716.
12. J.V. Beck, B. Blackwell and C.R. St. Clair, Inverse Heat Conduction, Wiley-Interscience Publication, New York, NY, 1985, 125-134;170-172.
13. T. Iida and R.I.L. Guthrie, The Physical Properties of Liquid Metals, Oxford University Press, Toronto, ON, Canada, 1988.

